# A Diquark Interpretation of the Structure and Energies of Hadrons

by

Alexander Selem

Submitted to the Department of Physics
in partial fulfillment of the requirements for the degree of

Bachelor of Science in Physics

at the

MASSACHUSETTS INSTITUTE OF TECHNOLOGY

June 2005





Author .....
Department of Physics
May 20, 2005

Certified by .....
Frank Wilczek
Professor of Physics
Thesis Supervisor

Accepted by .....
Professor David E. Pritchard
Senior Thesis Coordinator, Department of Physics

# A Diquark Interpretation of the Structure and Energies of Hadrons

by

Alexander Selem

Submitted to the Department of Physics
on May 20, 2005, in partial fulfillment of the
requirements for the degree of
Bachelor of Science in Physics

## Abstract

I present a simple phenomenological model which successfully organizes and classifies essentially all hadrons. The model is originally inspired from three simple theoretical indications including: treating baryons as a two body system with a diquark and quark connected by a flux tube, thereby indicating that they lie on Regge trajectories; allowing for independent combinations of diquark and quark to enumerate the observed trajectories; and that spin-flavor symmetric diquarks are more massive than their antisymmetric counterparts. With this framework essentially all hadrons can be consistently organized confirming the first three hypotheses and elucidating new ones, including: a universal slope or flux tube tension for both baryons and mesons implying the same color-charge at the flux tube ends, small spin forces external to diquarks, and the existence of tunneling effects. This framework and classification can then be used to estimate diquarks masses, and can be applied to exotic and cryptoexotic states. The model also make predictions for the existence of several particles and their energies; among them, tetraquark states. Finally, the arguments presented here naturally lead to many future projects in both experiment and theory.

Thesis Supervisor: Frank Wilczek
Title: Professor of Physics

# Acknowledgments

This work is the fruit of a collaboration with Frank Wilczek, and many of the ideas developed here were done so in conjunction. As my supervisor and mentor, I am most grateful to him for all the guidance, help, and wonderful exchange of ideas through countless conversations we have had.

I would also like to especially thank Robert Jaffe for many helpful discussions, and insights. I also benifited from discusions with Carlos Nuñez, Anthony Tagliaferro, and Barton Zwiebach.

This work was supported in part by the Paul E. Gray Endowed Fund, and I thank all those who have generously contributed to it.

Finally, I thank my family and God from which everything good has come. A.M.D.G.

# Contents

# Chapter 1

# Introduction and Background

The traditional quark theory of hadrons might be summarized as having two main inseparable components. The first describes the constituents of hadrons as being subparticles or quarks, as advanced by Gell-Mann in 1964 [1], while the second component is the theory describing how these interact, namely the relativistic field theory known as Quantum Chromodynamics (QCD). Each is elegantly and well described, and yet in practice this hardly seems to be the case. In what follows, I shall give a very brief summary of this practice as related to this work.

The rest of the work and the main goal of this thesis will be dedicated to advancing a model where objects called "diquarks" are elevated to play a central role in thinking about hadrons. In particular I shall first describe the motivations for diquarks, their implications in phenomenology and how well the experimental data supports these ideas. In doing so we shall find that a few simple hypotheses can be used to compactly classify essentially all hadrons, and give good predictions of their energies. Finally I shall discuss the many fruitful elaborations and extensions that arise from this classification and the diquark model in general.

Many of the ideas presented in this work will also elaborated upon in a work to be published [2].

## 1.1 Summary of the Uncorrelated Quark Model and Hadron Dynamics in Practice

As dictated by quantum field theories in general, the true structure of the hadrons is probably a "sea" of light quarks and massless gluons coming and going out of existence mediating the interaction of what are called valence quarks or those which are the minimal number necessary to define a given bound state or hadron. In terms of the sub-particle components of the hadrons, however, one can just think of the valence quarks as being the constituents of the hadrons, and take the rest to be part of the interactions between these. The quarks have colors, $r$, $b$, $g$ (an SU(3) symmetry), spin (an SU(2) symmetry), and flavors $u$, $d$, $s$, $c$, $b$, $t$, (which can be thought of as a very badly broken SU(6) symmetry, or an approximate SU(3) symmetry formed by $u$, $d$, and $s$). Because of the symmetry breaking in flavor it is sometimes intuitive to think of quarks of different flavors as inherently different. Yet being fermions, we must worry about symmetry under exchange, and in this regard flavor is treated as a perfect symmetry.

Mesons are (typically) described by a quark-antiquark pair ($q\bar{q}$), while baryons by three quarks ($qqq$). Most generally, any $q^{n_q}\bar{q}^{n_{\bar{q}}}$ combination is allowed as long as $n_q - n_{\bar{q}} = 0 \mod 3$, where $n_q$ is the number of valence quarks present and $n_{\bar{q}}$ antiquarks present. This is required by an empirical and theoretical (via asymptotic freedom) fact that all observed objects must be color singlets. In the traditional quark theory, the quarks in the hadron ground state are each in their lowest state, and particle excitations proceed by exciting each of the quarks one at a time. Finally, the quarks having spin, requires us to ensure that Fermi statistics are obeyed. In mesons, because the antiquark is inherently a different particle than the quark, issues of symmetry under exchange need not be considered. However, as baryons are made of "identical" quarks (here flavor symmetry is taken to be exact), we must have that $|color\rangle \times |flavor\rangle \times |spin\rangle \times |spatial\rangle$ be antisymmetric, where the ket refers to the whole baryon wave function, or the combined wave function of its three quarks. In particular because the color part is always antisymmetric, this requires $|flavor\rangle$

$\times$ $|spin\rangle$ $\times$ $|spatial\rangle$ to be symmetric. The symmetry of the spatial part is denoted by the particle's parity. The traditional quark model puts all quarks in the lowest excitation mode, where each has a positive or even parity while the antiquarks are given negative or odd parity. Baryons in their ground state, therefore, have even parity relative to the proton. Each quark (or antiquark in mesons) can then be separately excited by putting it in a higher energetic mode, having no effect on its parity, or by increasing in orbital angular momentum. Orbital excitations affect the parity according to $P = (-1)^L$, where $L$ is the orbital angular momentum of the state. For mesons another important quantity is charge conjugation $C$, given by $C = (-1)^{L+S}$, where $S$ is the total spin of the particle.

As mentioned, QCD is the theory that then describes how these quarks interact. The quark theory without QCD can only at best enumerate the states and quantum numbers of hadrons, but nothing can really be said as to the masses of the hadrons themselves or any other observables. Interesting predictions are only made when the dynamics of the quarks are taken into account. However, to date, no one has yet been able to systematically solve the QCD Lagrangian to produce an accurate description for the bound states of the quarks–namely the hadrons. Instead our true theoretical tests of QCD come from numerical super-computer calculations, which have been done in special cases; among these the ground states of observed hadrons–which are in remarkable agreement with experiment (for example see Ref. [3, 4]), thereby justifying our belief in the fundamental theory.

But this hardly suffices as a substitute for our understanding of hadrons. Instead many models have been employed in an attempt to dynamically describe hadrons. First there are non-relativistic potential models which treat the quarks as non-relativistic bodies in a potential governed by the Schrödinger equation [5, 6, 7, 8]. Typically a Coloumbic plus linear potential is used, $V(r_{ij}) = -a/r_{ij} + br_{ij}$, where $ij$ refers to any two quarks. It is a wonder that this program works even for the light quarks, as they are thought to have masses on the order of 100 MeV, which is comparable to the QCD coupling constant of 200 MeV, thereby requiring a proper relativistic treatment (for an interesting discussion see Ref. [9]). There are, of course, many modifications

made in these models attributed to relativistic affects helping to make them more plausible and better predictors.

The opposite approach is to treat the quarks as completely relativistic. This is the essence of bag models which place quarks in a "bag" with various boundary conditions and degrees of freedom depending on the sophistication sought (for example [10, 11, 12, 13, 14, 15, 16, 17, 18, 19]). In these models, the vacuum exerts pressure $B$ ("the so-called bag constant") on the bag providing for confinement, and the quark wave functions are then determined by solving the Dirac equation. Of course in practice, "bags" sometimes amount to spherical static cavities or other simplifications [11, 12, 14, 15, 16, 17].

Finally, another simple phenomenological model is that of the flux-tube or string-like model, used for mesons with orbital angular momentum [20, 21]. Here the QCD force between the quark and antiquark is approximated by a string, or flux tube acting like an effective string, with some constant tension connecting the quark and antiquark. Most importantly, this model naturally reproduces experimental data and lattice calculations [22, 23] where the energy squared of a particle, $E^2$, plotted against $L$ (orbital angular momentum) lie on straight lines (Regge Trajectories).

# Chapter 2

# The Case for Diquarks

Most generally a diquark is a two quark system. Because of confinement, it cannot exist in isolation, but rather might exist in combination with other quarks to form a bound color-antisymmetric state. For example, a baryon, being thought of as a diquark paired with quark, is the simplest example where they might exist. The idea of diquarks is probably as old as the quarks themselves. Gell-Mann makes mention of their possible existence in his original paper on the quarks in 1964 [1], and since then there has been a vast literature where people have used many models of hadron structure employing diquarks. I refer the interested reader to a nice review given by Anselmino [24]. Briefly, I will mention some of the most salient points. One extreme view, is where a diquark is thought of as a point particle. This view implies firstly that the various non-spatial parts of its wave function must be anti-symmetric between the two quarks that form it, and secondly it is treated as having no internal structure. But a much less stringent idea of a diquark, is simply one where two quarks are said to be "correlated". In the literature the most general definition of a correlation focuses only on a spatial criteria whereby a diquark is simply two quarks whose mean distance is smaller than the mean distance with any other quarks in the particle. However, another interpretation of "correlation" is one where the diquark wave function is separately antisymmetryzed as in the point-like conception of a diquark, but still assuming the diquark to be an object containing the structure of two quarks with some separation. This is the view assumed in this thesis. We think of

a diquark as an internal component of a particle, having a substructure formed by two quarks whose wave function is separately antisymmeterized according to Fermi statistics, but spatially being treated only approximately as a separate isolated particle. Remarkably, we shall see that even when there is no good reason to assume this approximation is valid, the particle is still well described by having this isolated diquark.

## 2.1 Classifying Diquarks

Without mentioning dynamics, I have already described a main difference between a simple traditional quark model and our diquarks model. Namely, in a baryon, rather than thinking about Fermi statistics for the three independent quarks we enforce Fermi statistics on the diquark separately. Of course, *a priori*, color antisymmetry is not a requirement for the diquark, since the diquark will not and cannot exist in isolation. However, one of the main indicators for the plausibility of diquarks is that there is an attractive channel in the color antisymmetric combination of two quarks. The one gluon exchange of this combination seems to indicate a color attractive force with about 1/2 the strength of quark anti-quark interaction [25, 12, 26]. In this channel the diquark as a whole appears to have the color of a lone antiquark. Essentially for both color or flavor taken as $SU(3)$ symmetries, we have $\mathbf{3}_{f,c} \otimes \mathbf{3}_{f,c} \rightarrow \bar{\mathbf{3}}_{f,c} \oplus \mathbf{6}_{f,c}$. This is shown graphically in Figure 2.1 making explicit the analogy of a diquark to an antiquark in color for the antisymmetric channel ($\bar{\mathbf{3}}_c$).

So from dynamics we assume that the diquark must always be antisymmetric in color, thereby implying $(|flavor\rangle \times |spin\rangle)_{diquark}$ to be symmetric (assuming the spatial parts contribute symmetrically). As such, a vector diquark (spin symmetric, $\mathbf{3}_s$) is always flavor symmetric $\mathbf{6}_f$ and the spin singlet diquark, $\bar{\mathbf{1}}_s$, is always flavor antisymmetric ($\bar{\mathbf{3}}_f$). Therefore it is fitting to distinguish between these two cases by simply writing the diquark having $(\bar{\mathbf{1}}_s, \bar{\mathbf{3}}_f)$ as $[qq']$ and the $(\mathbf{3}_s, \mathbf{6}_f)$ as $(qq')$. Here $q$ and $q'$ are most generally any two quarks. Although we have considered only the $SU(3)$ flavor, we might also extend these considerations to *any* quark (the whole

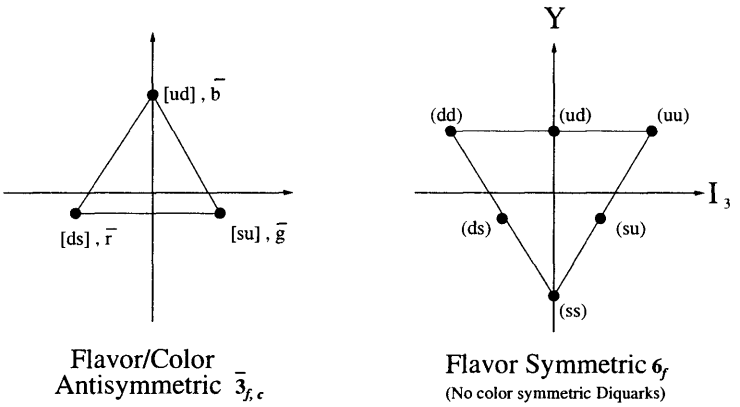


Figure 2-1: $SU(3)$ weight diagrams for the light diquarks. For the antisymmetric case, both flavor and and color is shown, explicitly making the correspondence in color between a diquark and an antiquark. (Adapted from Ref. [27])

$SU(6)$ group).

Once Again taking dynamical considerations into account we can say more about the distinction of a $[qq']$ diquark and a $(qq')$. For presumably there is also a color spin-spin interaction between the quarks in the diquark. Indeed many phenomenological models include a term of the form:

$$\mathcal{H}_{color-spin} \sim -\vec{\sigma}_i \cdot \vec{\sigma}_j \widetilde{\lambda}_i \cdot \widetilde{\lambda}_j, \tag{2.1}$$

where $\vec{\sigma}_i$ and $\widetilde{\lambda}_i$ are the Pauli and Gell-Mann matrices corresponding to the spin and color of the $i^{th}$ quark [27]. Such an interaction suggests that the vector diquark $(qq')$ has a greater mass than the singlet diquark $[qq']$. As such, it is helpful and appropriate to just call the $[qq']$ diquark, which has a favorable interaction, a "good" diquark and the $(qq')$ a "bad" diquark. We can go further in saying that because of relativistic effects, we expect lighter quarks to be more affected by this interaction than heavier quarks. That is, we expect a splitting of $(ud) - [ud] > (us) - [us] > (uc) - [uc] \approx 0$, where it should always be understood that $(qq') - [qq']$ is the difference of the diquark *masses* [1].

[1] I will later discuss in more detail plausible values for the masses of diquarks, as indicated from the classification of particles according to diquarks.

The simple distinction between bad and good diquarks, and allowing for different quark flavors exhausts the classification of diquarks I will consider in this thesis.

## 2.2 Motivations and Initial Hypotheses

I now begin to address the important question of whether diquarks are involved in baryonic structure. There have been many papers published investigating this possibility in the frame-work of non-relativistic potential models, as well as phenomenological models that naturally incorporate diquarks.

Firstly we consider what has been concluded mostly in the context non-relativistic potential theory. Of course we have no good reason to suppose that such conclusions are truly applicable. As case in point, Fleck et. al. [28], examined various reasons for which diquarks might be assumed to exist in baryons (in a potential model frame-work). They considered potentials of the form linear plus Coloumbic as described above (see Introduction and Background), and a power-law potential, $\sim r_{ij}^{\beta}$. They find by examining the wave function and looking for a spatial correlation, that only in cases of three light quarks ($qqq$) with high angular momentum ($L \approx 8$), or ($QQq$) with low angular momentum, do diquarks form. Here, $Q$ is referring to a heavy quark ($c$, $b$, $t$). Of course this is not all that surprising considering they are using perfectly symmetric potentials of the same form between all pairs of quarks (save for differences in quark masses). However, one cannot be certain that the non-relativistic limit is correct, and it is certainly plausible that the "potential" may have extra terms, in particular a very favorable spin-spin interaction with a different $r_{ij}$ dependence favoring the good diquark formation, especially for light quarks. Indeed where we can be sure the non-relativistic limit is correct, that is for heavy quarks, even for low $L$ diquarks form.

Contrarily the findings of Martin [29] show, under the context of potential theory, that the minimal energy state for baryons *is* a quark-diquark system and that their orbital angular momentum excitations lie on linear Regge trajectories with the same slope as mesons.

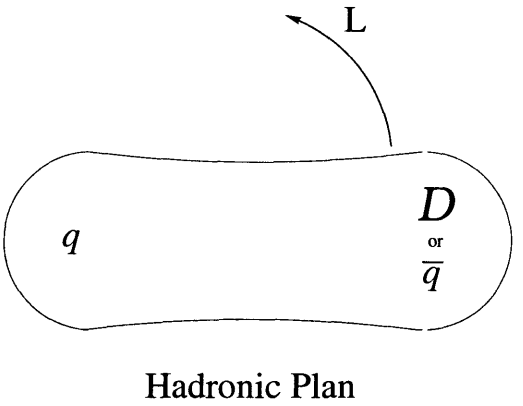


Figure 2-2: The typical rotating model for any hadron. Here "D" stands for diquark.

However, the most suggestive evidence for diquarks comes some from several phenomenological indications. These include regularities in parton distribution functions, and in the $\Lambda$ fragmentation function [2, 27].

Finally because of their simplifying role, several phenomenalogical models have used diquarks. In particular, in the context of bag models, an obvious possibility is to model high angular momentum baryons as an extended flux tube with a diquark at one end and a quark on the other, as is done with mesons. Since 1975, Johnson and Thorn [20] examined this possibility in a flux-tube type bag, which can be treated as a string of constant tension whose value can be related to the fundamental bag parameters such as the "bag constant" $B$, and the strong coupling constant $\alpha_c$. Iwasaki et. al. [30, 31] undertook a similar program but postulating a "multibag" model where the diquark was placed into a separate internal bag (and the lone quark into it's own bag). As motivation for this, they separately calculate the masses of each bag, assuming little interaction between them, and then show that the masses of both separate bags sum to less than the one entire bag. The main difficulty with this reasoning, however, is that they use energy terms from Ref. [12] that were derived with a color confining boundary condition–a condition that is not realizable in a bag with a single quark/antiquark or diquark.

Nevertheless it is in the spirit of these phenomenological models, that we picture a rotating baryon as a two body plan as shown in Figure 2.2. The particle can be

thought as a spinning flux tube or string of constant tension $T$ (remarkably despite what thickness it may have), and integer-quantized angular momentum. Although such models were used in the past to explain general Regge-Trajectories observed in the baryon sectors with some success, we show that by making some other simple assumptions, essentially all hadrons can be consistently well organized and explicitly classified.

In particular the classification was first guided by considering several initial hypotheses motivated from arguments like those already discussed. After the classification was achieved, the hypotheses were confirmed and more generally modified, and new ones were also learned, in extraordinary consistency with a diquark interpretation of baryons. I shall outline these final hypotheses in the next section. Explicitly, the initial hypotheses were (explanations to follow):

1. Baryons, at least with large total angular momentum $L \geq 4$ (quantized in integers), can be thought as being made of a diquark and quark in a rotating two body plan as described.

2. The dynamical two body model, implies that sets of resonances having the same internal quantum numbers (spins at the ends), lie along trajectories (Regge trajectories) of the form:

$$M^2 = a + \sigma L. \tag{2.2}$$

   This is the well know Chew-Frautschi relation. Here $M^2$ is the mass-squared of the hadron ($M$ will be used interchangeably with the energy $E$), $\sigma$ is a slope universal for all Regge trajectories, while $a$ varies for each trajectory as defined by the spins at the hadronic ends (including the distinction between good and bad diquarks).

3. The degrees of freedom at the end of the hadron are weakly coupled to each other.

4. There is some expected difference in mass between a good and bad diquark. In $M^2$ vs $L$ space, this suggests $a$ to be greater for a trajectory containing a bad

diquark as opposed to a good one.

## 2.3 Developed Hypotheses

All baryons were organized taking into account the "initial hypotheses". However as will be shown, upon classifying the hadrons, much was learned and the hypotheses evolved into a more developed set that can exhibited in the data. These ideas are summarized as the following "developed" hypotheses and are to be taken as what we will conclude in this work:

1′. The diquark with quark model for baryons, in a two body or at least effective two body plan, is valid down to $L \rightarrow 0$.

2′. The Chew-Frautschi relationship extends down to $L = 0$. And so all baryons lie on Regge trajectories, with $a$ different for good and bad diquarks. The mesons can also be shown to lie on similar trajectories, and there is a universal slope for both mesons and baryons.

3′. As we postulated originally, the degrees of freedom at the ends of the hadrons are indeed weakly coupled. However we shall find that for both small or large $L$, there may be overlap between wave functions. The only evidence of this is manifested in the tunneling by a quark from a diquark to the other side. This gives rise to a so-called "even-odd" effect exhibited only in certain symmetric cases where they should be. Thus we have a model where wave functions may overlap, but dynamically and for purposes classification they behave as though they do not, except for an expected and seen even-odd effect in some cases.

4′. Bad diquarks are clearly more massive than good diquarks. In $E^2$ vs $L$ space, this represents a larger $a$ (Regge intercept) for bad diquarks. In general different diquarks will imply different $a$ values. From the semi-classical model of the rotating baryons and by classifying and comparing mesons, we can extract effective masses for diquarks and quarks.

5′. A simple generalization of the Chew-Frautschi relation gives for heavy-light quark/diquark systems:

$$(M-\mu)^2 = a + \frac{\sigma}{2}L, \tag{2.3}$$

where $\mu$ is the mass of the heavy end, and $\sigma$ is the same universal slope.

6′. Spin interactions, besides those found internally within diquarks, are negligible.

## 2.4 Explanations of the Hypotheses

The two body plan in the first hypothesis was motivated for large $L$. We must simply let the experimental data dictate to us that it is universally valid for all $L$, or at least an effective two body plan is valid. It's validity is tested indirectly through the simple dynamical semi-classical model of the spinning flux-tube or string of constant tension $T$, since such a model implies the Chew-Frautschi relation. In what follows we will exhibit the general relation between the energy $E$ and $L$, for spinning string of constant tension $T$ and arbitrary masses at its end. When the masses are light, or the string rotates rapidly, the quoted Chew-Frautschi is reproduced perfectly. Specifically the slope $\sigma$ is related to the string tension by $\sigma = 2\pi T$. Hence because this is observed at all $L$, we must assume that even for small angular momentum an effective two body system approximately holds.

Furthermore because the tension presumably arises from the color flux between the string/flux tube ends, a universal slope including those of the meson sectors implies that the same color charges reside in the baryon string ends, (i.e. the diquarks are there and they are anti-symmetric in color as discussed).

As will be shown, a pure string with massless ends leads to the relation $E^2 = \sigma L$. One might wonder what the proper interpretation of the observed Regge trajectory intercept, $a$, is. Strictly adhering to the classical string picture the only hope is to make the ends of the strings massive. Of course, as is shown in the following section, this introduces some non-linearity in $E^2$ vs $L$ space for very small $L$, between 0 and 1, which is not observed for quantized $L$. Still this would posit a deviation from

linearity between the ground state (defining the intercept) and $L = 1$, so that one would have to argue quite naturally that a breakdown of the simple string model with point masses might occur but conspires to keep things linear when matching $L = 1$ with 0. For one thing the mass distribution and short-range interaction between the ends should affect the model. In this interpretation, the existence and observed differences in $a$ could be explained quite naturally by differences in the non-negligible effective masses for the different quarks and diquarks. The details of this possibility will further be discussed in the following section.

Finally, a second approach to explain the intercept, might posit the existence of some zero-point quantization effect in terms of angular momentum. Namely their might be some overall non-zero $L$ manifest through the intercept. For example if $L_o = 0$, goes to $L'_o \rightarrow L_o + a'$, the massless string trajectory is shifted to $E^2 = \sigma L + \sigma a'$. Variations in the actual $a$ could then be explained again by variations in quark/diquark masses, but requiring the actual values to be much smaller, thereby preserving the linearity of the Regge trajectory which is recovered perfectly in the massless case.

The calculation for a string of the same tension but having one end very massive, gives the relation between $(E - \mu)^2$, the mass of the particle without the heavy end, squared, and $L$, as being linear with a slope $\pi T$, or half that of the slope for the light hadrons. This is seen experimentally for heavy-quark baryons, thereby implying the same universal tension for those as well.

Finally we note that the classification of the particles imply small spin-orbit forces. It has been suggested [2] that taking an interaction term as the fourth component of a vector leads to a term of the form $\sim \vec{\sigma} \cdot \vec{L}$. But if one treats the potential as a scalar, a similar term but opposite in sign results, thereby implying the potential to be taken as vector$^0$ + scalar.

### 2.4.1 Generalization of the Chew-Frautschi Formula

We can generalize the Chew-Frautschi formula by considering two masses $m_1$, $m_2$ connected by a "string" with constant tension, $T$, rotating with angular momentum

$L$. Our general solution will take a parameterized form in which the energy, $E$, and $L$ are both expressed in terms of the angular velocity, $\omega$, of the rotating system. In the limit that $m_1$, $m_2 \to 0$, the usual Chew-Frautschi relationship where $E^2 \propto L$ can be recovered. Other cases of interest in which analytic solutions of $E^2$ vs $L$ can be found are those when one mass is infinitely heavy and the other is approximately zero, or when both are infinitely heavy.

One can begin by considering the masses $m_1$ and $m_2$ distances $r_1$ and $r_2$ away from the center of rotation respectively. As implied, the whole system spins with angular velocity $\omega$. It is also useful to define in the usual manner:

$$\gamma_i = \frac{1}{\sqrt{1-(\omega r_i)^2}} \tag{2.4}$$

where the subscript $i$ can be 1 or 2 (for the mentioned masses). Then it is straightforward to write the energy of the system:

$$E = m_1\gamma_1 + m_2\gamma_2 + \frac{T}{\omega}\int_0^{\omega r_1} \frac{1}{\sqrt{1-u^2}}du + \frac{T}{\omega}\int_0^{\omega r_2} \frac{1}{\sqrt{1-u^2}}du. \tag{2.5}$$

The last two terms are associated with the energy of the string. Similarly the angular momentum can be written as:

$$L = m_1\omega r_1^2\gamma_1 + m_2\omega r_2^2\gamma_2 + \frac{T}{\omega^2}\int_0^{\omega r_1} \frac{u^2}{\sqrt{1-u^2}}du + \frac{T}{\omega^2}\int_0^{\omega r_2} \frac{u^2}{\sqrt{1-u^2}}du. \tag{2.6}$$

Carrying out the integrals gives:

$$E = m_1\gamma_1 + m_2\gamma_2 + \frac{T}{\omega}(\arcsin[\omega r_1] + \arcsin[\omega r_2]), \tag{2.7a}$$

$$\begin{aligned} L = {} & m_1\omega r_1^2\gamma_1 + m_2\omega r_2^2\gamma_2 \\ & + \frac{T}{\omega^2}\frac{1}{2}\left(-\omega r_1\sqrt{1-(\omega r_1)^2} + \arcsin[\omega r_1] - \omega r_2\sqrt{1-(\omega r_2)^2} + \arcsin[\omega r_2]\right). \end{aligned} \tag{2.7b}$$

Furthermore for each mass, the following relationship between the tension and angular acceleration must hold:

$$m_i\omega^2 r_i = \frac{T}{\gamma_i^2}. \tag{2.8}$$

We can use this to do away with the distances $r_1$ and $r_2$ and express everything in terms of $\omega$. Specifically we note that in our expressions for $E$ and $L$, the quantities that contain $r_i$, are $\gamma_i$ and also $\omega r_i$. From equation 2.8 we can ultimately solve for $\gamma_i$:

$$\gamma_i = \sqrt{\frac{1}{2} + \frac{\sqrt{1 + 4(T/(m_i\omega))^2}}{2}}. \tag{2.9}$$

And finally from equation 2.8 we also know that $\omega r_i$ is just $T/(m_i\gamma_i^2\omega)$.

We are now in a position to replace these terms in equation 2.7 and write $E$ and $L$ in terms of the parameter $\omega$ and other quantities known by definition, namely the masses and the string tension $T$. To this effect, perhaps the most useful way to write the expressions is to define another variable $x_i \equiv \frac{m_i\omega}{T}$ which can later serve as an expansion parameter for small masses $m_i$ (or large $L$). Making replacements into equation 2.7 we obtain:

$$E = \sum_{i=1,2} m_i \sqrt{\frac{1}{2} + \frac{\sqrt{1+x_i^2/4}}{x_i}} + \frac{T}{\omega} \arcsin\left[\frac{1}{x_i\left(\frac{1}{2} + \frac{\sqrt{1+x_i^2/4}}{x_i}\right)}\right] \tag{2.10a}$$

$$L = \sum_{i=1,2} \frac{T}{\omega_i^2} \frac{1}{x_i\left(\frac{1}{2} + \frac{\sqrt{1+x_i^2/4}}{x_i}\right)^{3/2}} + \tag{2.10b}$$

$$\frac{T}{\omega_i^2}\frac{1}{2}\left(-\frac{1}{x_i\left(\frac{1}{2} + \frac{\sqrt{1+x_i^2/4}}{x_i}\right)}\sqrt{1 - \frac{1}{x_i^2\left(\frac{1}{2} + \frac{\sqrt{1+x_i^2/4}}{x_i^2}\right)^2}} + \arcsin\left[\frac{1}{x_i\left(\frac{1}{2} + \frac{\sqrt{1+x_i^2/4}}{x_i}\right)}\right]\right).$$

While it may difficult to gain insight from these expressions, we can actually make much use of them by either parametrically plotting $E^2$ vs $L$ (C-F plot) for whatever values of $m_1$, $m_2$, and $T$ desired, or if we are considering either very light or very heavy masses, appropriate expansions can be made to obtain analytic expressions for $E^2$ vs $L$.

With regard to making appropriate expansions, it is important to note that the terms associated with each mass are completely decoupled from each other, as the

expressions involve just a sum of contributions from each mass. Hence, one can make expansions for any given mass up to the necessary order, or with whatever parameter (depending on whether the mass is very heavy or very light, where this approach makes sense). In light of this it is reasonable to talk about the contribution of a single mass to $E$ or $L$ without regard for the other. Hence we'll adopt a convention that denotes the contribution from one mass by a $\delta$, as in $\delta E$ in what follows. In particular if a given mass $m_i$ is very light or for large $L$, then as suggested $x_i$ serves as a good expansion parameter. If we expand in $x_i$, then, we find the contribution to the energy, $\delta E$, and angular momentum, $\delta L$, due to one light mass in this case would be (carried out to order $x_i^{5/2}$):

$$\delta E_{light} = \frac{\pi T}{2\omega} + \frac{1}{3}\left(\frac{\omega}{T}\right)^{1/2} m_i^{3/2} + \frac{1}{20}\left(\frac{\omega}{T}\right)^{3/2} m_i^{5/2} - \frac{3}{224}\left(\frac{\omega}{T}\right)^{5/2} m_i^{7/2} + O\left(m_i x_i^{7/2}\right) \tag{2.11a}$$

$$\delta L_{light} = \frac{\pi T}{4\omega^2} - \frac{1}{3}\frac{m_i^{3/2}}{(\omega T)^{1/2}} + \frac{3}{20}\frac{\omega^{1/2} m_i^{5/2}}{T^{3/2}} + O\left(\frac{T x_i^{7/2}}{\omega^2}\right). \tag{2.11b}$$

For a system with two light and equal masses, we would of course just multiply the right hand side of these expressions by two to obtain the total energy and angular momentum. Also note that at least for a very light mass it seems that as $L \to 0$, $\omega \to \infty$ and taking this limiting case in the general expressions shows that this is indeed the case. As such, care must be taken to make sure that the expansions are valid depending on $L$ values. In practice therefore it is much more useful to look at parametric plots at least as a check. However, if we let both masses go to zero, and therefore take only the first term for each mass from the light-mass expansion (equation 2.11), then the we recover the familiar Chew-Frautschi relationship for the string with massless ends:

$$E^2 = (2\pi T)L. \tag{2.12}$$

Of course, a different regime is that where one or both masses become infinitely heavy. In this case, we might instead expand terms for a given mass with a parameter $\frac{1}{x_i} \equiv \frac{T}{m_i \omega}$. As before we can expand the contribution from one mass, but this time a

heavy one, as follows (expanded to 4th order in $1/x_i$):

$$\delta E_{heavy} = m_i + \frac{3}{2}\frac{T^2}{m_i\omega^2} - \frac{35}{24}\frac{T^4}{m_i^3\omega^4} + O\left(\frac{m_i}{x_1^6}\right) \tag{2.13a}$$

$$\delta L_{heavy} = \frac{T^2}{m_i\omega^3} - \frac{7}{6}\frac{T^4}{m_i^3\omega^5} + O\left(\frac{T}{\omega^2 x_i^5}\right). \tag{2.13b}$$

Using these expansions one can easily find the analytic solution for the case of one very heavy mass $M$ connected to a light mass (approximately zero). Specifically for the heavy mass contribution we can take just the first term for the energy and none for the angular momentum from equation 2.13; and the first terms of equation 2.11 for the contributions of the light mass. This would give the expressions:

$$E = M + \frac{\pi T}{2\omega} \tag{2.14a}$$

$$L = \frac{\pi T}{4\omega^2}, \tag{2.14b}$$

which ultimately yields the relationship:

$$(E - M)^2 = \pi T L. \tag{2.15}$$

Hence we see that the C-F relationship for a heavy-light mass system is the same as the two-light-masses case but with *half the slope* and with the energy shifted by that of the heavy mass.

In reality, however, many interesting examples fall between these mentioned limiting cases. As already suggested, to see the behavior of all these other cases, we must simply examine parametric plots of expression 2.10. Doing so one finds that for a robust range of masses, the extremal cases are well approximated. Several of these plots are presented in appendix A.

# Chapter 3

# The Classification of Particles

## 3.1 Methods

In practice, classifying the particles involves first listing the possible diquark-quark states and searching out candidates based on their energies, total angular momentum, and parity. For sectors containing few particles, this program is not very difficult. However, the formidable nucleon-delta complex with its plethora of particles may present an interpretive challenge. To handle such a case, and in the future as more particles are discovered, I will outline a visual and intuitive method to aid in the classification.

To classify the particles "visually", one should plot the particles from a given complex in $E$ vs $L$ ($J$, total angular momentum also implied), differentiating between particles and their parity. Figure 3-1 (on the left) shows this for the nucleon-delta complex. Note, that only resonances having 2* or better rating according to the Particle Data Group (PDG) [32] are plotted and considered throughout this work. The goal is then to establish what I shall call the "constant-L" diagram for the sector. As the name suggests this is a diagram which groups all particles with a given angular momentum in $E$ vs $L$ space. The diagram will have some approximate geometric shape whose vertices are the corresponding particles for that given $L$. Thus the classification then becomes a simple matter of visually identifying this shape in the plot containing all particles.

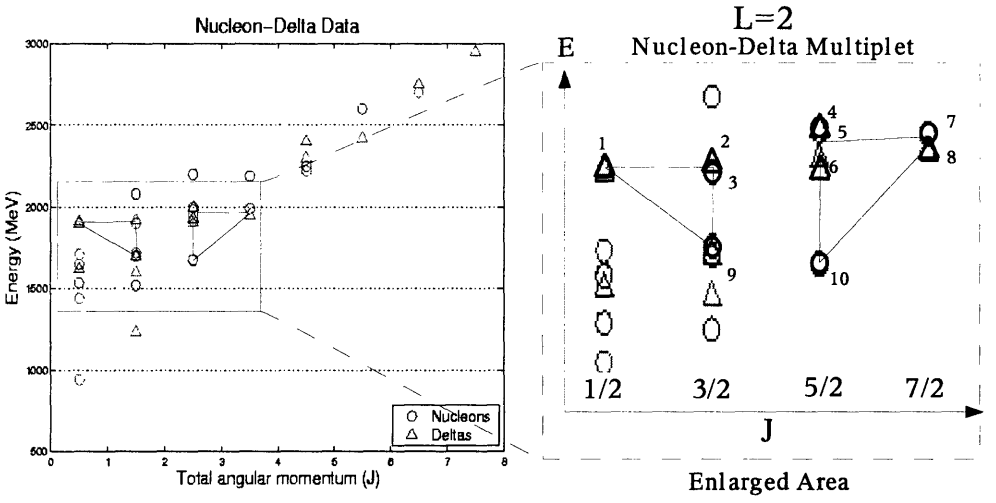


Figure 3-1: Multiplet of nucleon-deltas with $L = 2$, as taken from the data plotted on the left. In practice the particles are easily grouped based on parity. The numbered particles identified as $L = 2$ on the right correspond to **1** $\Delta(1910)$, **2** $\Delta(1920)$, **3** $N(1900)$, **4** $\Delta(2000)$, **5** $N(2000)$, **6** $\Delta(1905)$, **7** $N(1990)$, **8** $\Delta(1950)$, **9** $N(1720)$, **10** $N(1680)$.

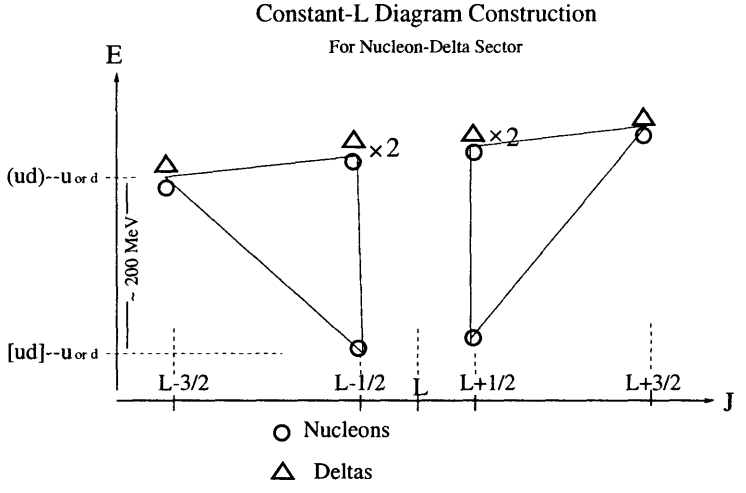


Figure 3-2: Shown here is the expected multiplet of nucleons and deltas for a given value of $L$ plotted linearly in energy versus total angular momentum. The diagram can be constructed first by considering the possible quark contents and noting the hypothetical separation in their energies, thus creating the two rows as well as determining what particles are allowed in each row. Finally for a given quark content, the different allowed spin configurations are considered. Note that depending on the spin interactions, the rows may have a slope as shown. Also note that a different diagram is to be expected for every sector.

To find the diagram, which will be different for every sector, we first label on the energy axis the diquark-quark combinations that are possible in that sector. Here one must make a prediction between the relative energy difference between the diquarks. The idea is just to postulate some ordering and energetic spacing between the different diquark-quark constituents in the sector. For the nucleon-delta sector this is shown in Figure 3.2. Next, one labels the center $L$ for the graph and considers the different spin states that the quarks and diquarks may take and whether they are aligned or not. In the limit of no spin-dependent forces, the particles with different spins are all equivalent in energy and should therefore lie on a horizontal line from the energy of its respective diquark. For greater spin forces, the lines for increasing total $L$ should be upward sloping. Again the example for the nucleon-delta sector is shown. Note the manifestation of hypothesis 6′: that the spin-dependent forces outside of diquarks are indeed feeble. Also note that these considerations determine not only the possible shape, but what particles can be found where. In this example the good diquarks can only have total $L$ of only $L \pm \frac{1}{2}$:

$$L \otimes \frac{1}{2} = (L + \frac{1}{2}) \oplus (L - \frac{1}{2}). \tag{3.1}$$

Bad diquark-containing particles, contain particles from $L - \frac{3}{2}$ to $L + \frac{3}{2}$:

$$L \otimes 1 \otimes \frac{1}{2} = (L + \frac{3}{2}) \oplus (L + \frac{1}{2}) \oplus (L + \frac{1}{2}) \oplus (L - \frac{1}{2}) \oplus (L - \frac{1}{2}) \oplus (L - \frac{3}{2}) \tag{3.2}$$

(with of course the understanding that negative values are to be dropped). Furthermore in terms of isospin, the bad diquark has isospin 1 (flavor symmetric, as discussed above), which can be paired with the isospin $\frac{1}{2}$ quark to give both nucleons and deltas essentially degenerate.

Once this multiplet with the same $L$ can be identified, then it can be matched to the particles in the whole plot, which in practice can easily be done by identifying particles of the same parity as shown in Figure 3-1. Also the center of the multiplets should rise for the different $L$, according to $E \propto \sqrt{L}$.

For most of the other sectors, this visual method of classification is probably

unnecessary given the sparseness of the present data, however, it provides a good template for classifying future discoveries. Also, we must not forget that while classifying the particles in this way may help distinguish between possible ambiguities, for the purposes of the following analysis we are actually not interested in particles of the same angular momentum, but in the set of different angular momenta for particles having the same quantum numbers (i.e. the Regge trajectories). These sets can then be plotted in in $E^2$ vs $L$ and fitted according to the Chew-Frautschi relationship. What follows presents the classification of all baryons established by the PDG [32] with 2* or better, and all mesons marked by a dot (•).

## 3.2 The Light Baryons

### 3.2.1 Nucleon-Delta Complex

The classification of essentially all nucleon-delta particles are shown in Table 3.1. This table and all others from here on are divided into series, designated by Roman numerals, representing the different possible net spin alignments. These are further divided into the possible ways of obtaining the net spin alignment, and they are denoted by letters. Furthermore we adopt the graphical convention of a simple dash $(-)$ for a spin singlet and a double arrow for a vector diquark (such as $\Uparrow$ or $\Leftrightarrow$). Arrows pointing up are aligned, and down anti-aligned. Also we generically label an isospin $\frac{1}{2}$ quark ($u$ or $d$) simply as $l$, unless they are found paired as a good diquark in which case they are explicitly written, $[ud]$, and understood to be antisymmetric. The first series assumes maximal alignment between orbital and spin angular momentum. For $L = 0$ there is a unique nucleon state, since (assuming spatial symmetry) spin symmetry and color antisymmetry imply flavor symmetry. For larger values of $L$ there is both a good diquark and a bad diquark nucleon state. The latter is made by assembling the $I = 1$ bad diquark with the $I = \frac{1}{2}$ quark to make $1 \otimes \frac{1}{2} \rightarrow \frac{1}{2}$. According to hypothesis 3′, independence of the two ends, we should expect to have approximately degenerate bad diquark nucleons and deltas. Examples of this include

Table 3.1: Nucleon-Delta Classifications. Particle masses taken from the Particle Data Tables [32] with the $J^P$ convention. $l$ represents either a $u$ or $d$ quark.

**I. Maximal spin alignment for "Good" and "bad" diquarks.**

| *Angular Momentum* ($L$) | **A. [ud]—l** ——↑ | **B. (ud)—l** ⇑—↑ | |
|---|---|---|---|
| 0 | $N(939)$ $1/2^+$ | $\Delta(1232)$ $3/2^+$ | - |
| 1 | $N(1520)$ $3/2^-$ | | $N(1675)$ $5/2^-$ |
| 2 | $N(1680)$ $5/2^+$ | $\Delta(1950)$ $7/2^+$ | $N(1990)$ $7/2^+$ |
| 3 | | $\Delta(2400)$ $9/2^-$ | $N(2250)$ $9/2^-$ |
| 4 | $N(2220)$ $9/2^+$ | $\Delta(2420)$ $11/2^+$ | |
| 5 | $N(2600)$ $11/2^-$ | $\Delta(2750)$ $13/2^-$ | |
| 6 | $N(2700)$ $13/2^+$ | $\Delta(2950)$ $15/2^+$ | |

**II. One "unit" less then maximal spin alignment.**

| *Angular Momentum* ($L$) | **A. [ud]—l** ——↓ | **B. (ud)—l** ⇑—↓ or ⇔—↑ | |
|---|---|---|---|
| 1 | $N(1535)$ $1/2^-$ | $\Delta(1700)$ $3/2^-$ | $N(1700)$ $3/2^-$ |
| 2 | $N(1720)$ $3/2^+$ | $\Delta(1905)$ $5/2^+$ | $N(2000)$ $5/2^+$ |
| | | $\Delta(2000)$ $5/2^+$ | |
| 3 | | | $N(2190)$ $7/2^+$ |
| 4 | | $\Delta(2300)$ $9/2^+$ | |

**III. Two "units" less then maximal alignment.**

| *Angular Momentum* ($L$) | **A. (ud)—l** ⇓—↑ or ⇔—↓ | |
|---|---|---|
| 1 | $\Delta(1620)$ $1/2^-$ | $N(1650)$ $1/2^-$ |
| 2 | $\Delta(1920)$ $3/2^+$ | $N(1900)$ $3/2^+$ |
| 3 | | $N(2200)$ $5/2^-$ |

**IV. Maximal "bad" diquark anti-alignment.**

| *Angular Momentum* ($L$) | **A. (ud)—l** ⇓—↓ | |
|---|---|---|
| 2 | $\Delta(1910)$ $1/2^+$ | |
| 3 | | $N(2080)$ $3/2^-$ |

the $\Delta(1950)\ \frac{7}{2}^+$ with the $N(1990)\ \frac{7}{2}^+$ in the first series, the $\Delta(1920)\ \frac{3}{2}^+$ with the $N(1900)\ \frac{3}{2}^+$ in the third series, and some other more corrupted pairs. In general, the existence of a second nucleon series corresponding to a bad diquark is direct implication of this diquark model with weakly coupled degrees of freedom, rather than one whole antisymmetric nucleon ground state. Furthermore there seems to be a clear energetic distinction between good and bad diquarks of about 200 MeV as can be seen by comparing the first and third columns of the series.

Classifying the particles in this manner also shows that their are particles yet to be discovered. In particular the predictions can be made for the existence in the first series of a $N(2000)\ \frac{7}{2}^-$ and a $\Delta(1700)\ \frac{5}{2}^-$. Also the $\Delta(2400)\ \frac{9}{2}^-$ is relatively high in mass and thus we would expect it to be about $\approx$ 100 MeV lighter.

The second series includes cases where the spin and orbital angular momenta sum up to one less than the maximum possible $J$. We do not expect any states for $L = 0$ since with no separation of the two ends, the bad diquark formation is unfavored. Note that in that in the second two columns of this series there are two possible spin alignments (see the decomposition in the 3rd paragraph of the "methods" subsection). Thus there should be a degenerate state for particles here. Only one possible candidate pair is found: the $\Delta(1905)\ \frac{5}{2}^+$ $\Delta(2000)$ and $\frac{5}{2}^+$, of which we predict that the $\Delta(1905)$ is too low.

Finally recall as previously mentioned the feebleness of spin forces, most amply seen at the $L = 2$. We find two nearly degenerate good-diquark nucleons $N(1680), N(1720)$ with $J^P = \frac{5}{2}^+, \frac{3}{2}^+$; and a host of nearly degenerate bad-diquark nucleons and deltas $N(1990)\ \frac{7}{2}^+$, $N(2000)\ \frac{5}{2}^+$, $N(1900)\ \frac{3}{2}^+$, $\Delta(1950)\ \frac{5}{2}^+$, $\Delta(1905)\ \frac{5}{2}^+$, $\Delta(2000)\ \frac{5}{2}^+$, $\Delta(1920)\ \frac{3}{2}^+$, $\Delta(1910)\ \frac{1}{2}^+$.

We now begin to consider the evidence for the Regge Trajectories implied in hypotheses 1 and 2. In particular, series IA and the deltas of IB, are most represented. However, upon plotting these, we find a most consistent pattern: that the odd-$L$ particle have more energy than their even-$L$ partners. This so called "even-odd" effect is shown explicitly in Figure 3.3. A possible explanation for this effect might be that the a quark from the diquark can tunnel out to the other side of the particle. Thus

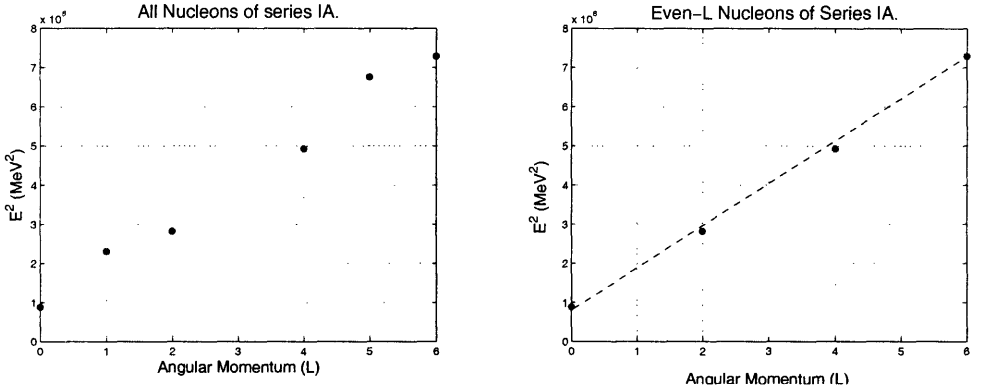


(a) (b)

Figure 3-3: (a) Plot of nucleons showing "even-odd effect". (b) Just the even-L where the trajectory is truly linear. Dashed line shown for reference.

Figure 3-4: Symmetric hadron with tunneling quark to produce the same baryon rotated by $\pi$.

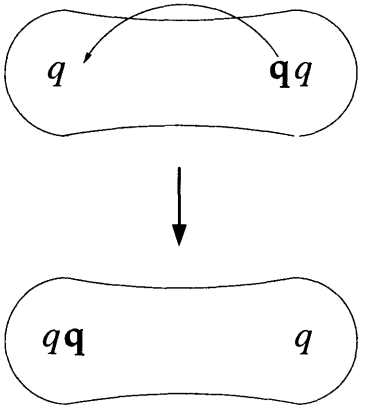

for certain symmetric cases such as in the nucleon-delta sector such a tunneling would amount to a rotation of a fixed bone through $\pi$ as shown in Figure 3.4. Therefore we should construct spatial wave functions that are symmetric or anti-symmetric under this exchange. The symmetric case, would be node-less and therefore have less energy, while the opposite is true for the antisymmetric case. The even $L$ would correspond to the symmetric case while the odd $L$ to the antisymmetric one. Hence we should expect that when tunneling of this kind is significant, there be some separation between the even and odd $L$. We can say something more quantitative about this effect, but will relegate that discussion to its own section following the classification of the other baryons.

When the even-odd effect is accounted for by separating out the series into even and odd $L$, the trajectories are very linear as predicted. Table 3.2 shows the observed values for all classified series. Note that many series are sparse and contain just two points which trivially make a line and gives a poor estimate for the universal slope. Nevertheless many of these are still in surprising agreement. If we consider the most prominent trajectories, the picture is even more consistent. The values for these are isolated in Table 3.3. We find an average slope from these of 1.18 $\text{GeV}^2$. Finally plots for the more prominent fits of all the classifications are shown in Figure 3.5 and should serve the reader as a reference in the following sections.

### 3.2.2 Other Light Baryons

Tables 3.4 and 3.5 show the bulk of our classifications for all other light hadrons (no nucleon-deltas). First we consider the lambda-sigma sector or baryons containing two light one strange quark $(lls)$. Four possible diquark configurations come into play: $[ud]$, $(ll)$, $[ls]$, $(ls)$. Since the $[ud]$ diquark is so favorable we would expect it to be well represented, and indeed we find a very clear trajectory from $L = 0$ to $L = 5$ of $\Lambda$ baryons in the first series. In this trajectory we predict that the spin-parity of $\Lambda(2350)$, which is debated, should be $\frac{9}{2}^+$, while that of $\Lambda(2585)$ should be $\frac{11}{2}^-$. In general all particle classified with unknown spin-parity may be regarded as predictions of the classification. The linearity of this trajectory, as shown in Figure 3.2.1(c), is

Table 3.2: Listed here are *all* the fitted slopes and intercepts for all series corresponding to light hadrons; including those with two just points. Note that even many of these are quite consistent in their slope! "Sector" refers to the hadron type which can be found in tables 3.1 to 3.7. "Series" corresponds to the different Regge trajectories as labeled in the respective tables. The parameters correspond to a fit of the relation $E^2 = \sigma L + a$.

| Sector | Series | points in series | $\sigma$ (GeV$^2$) | $a$ (GeV$^2$) |
|---|---|---|---|---|
| nucleons | IA. even | 4 | 1.07 | .781 |
| nucleons | IA. odd | 2 | 1.112 | 1.198 |
| nucleons | IB. odd | 2 | 1.128 | 1.677 |
| nucleons | IIB. odd | 2 | .953 | 1.937 |
| nucleons | IIIA. odd | 2 | 1.059 | 1.664 |
| deltas | IB. even | 4 | 1.18 | 1.429 |
| deltas | IB. odd | 2 | .901 | 3.056 |
| deltas | IIB. odd | 2 | .738 | 2.339 |
| lambdas | IA. | 6 | 1.08 | 1.211 |
| sigmas | IB. even | 3 | 1.15 | 1.404 |
| sigmas | IB. odd | 3 | 1.09 | 1.849 |
| sigmas | IC. even | 2 | 1.101 | 1.919 |
| cascades | IA. even | 3 | .969 | 1.779 |
| rho/a | IA. | 6 | 1.13 | .6444 |
| rho/a | IIIA. | 2 | .788 | 1.325 |
| omega/$f$ | IB. | 5 | 1.16 | .5527 |
| omega/$f$ | IIIB. | 3 | 1.082 | .7166 |
| phi/$f$ | IC. | 3 | 1.19 | 1.072 |
| phi/$f$ | IIIC. | 2 | 1.35 | 1.09 |
| pi/$b$ | IIa singlet | 3 | 1.385 | .0599 |
| eta | IIbA singlet | 3 | 1.20 | .2574 |
| eta$'$ | IIbB singlet | 2 | .983 | .9216 |
| kaon | I. | 5 | 1.19 | .7962 |
| kaon | II. | 5 | 1.56 | .229 |
| kaon | III. | 2 | .778 | 1.267 |

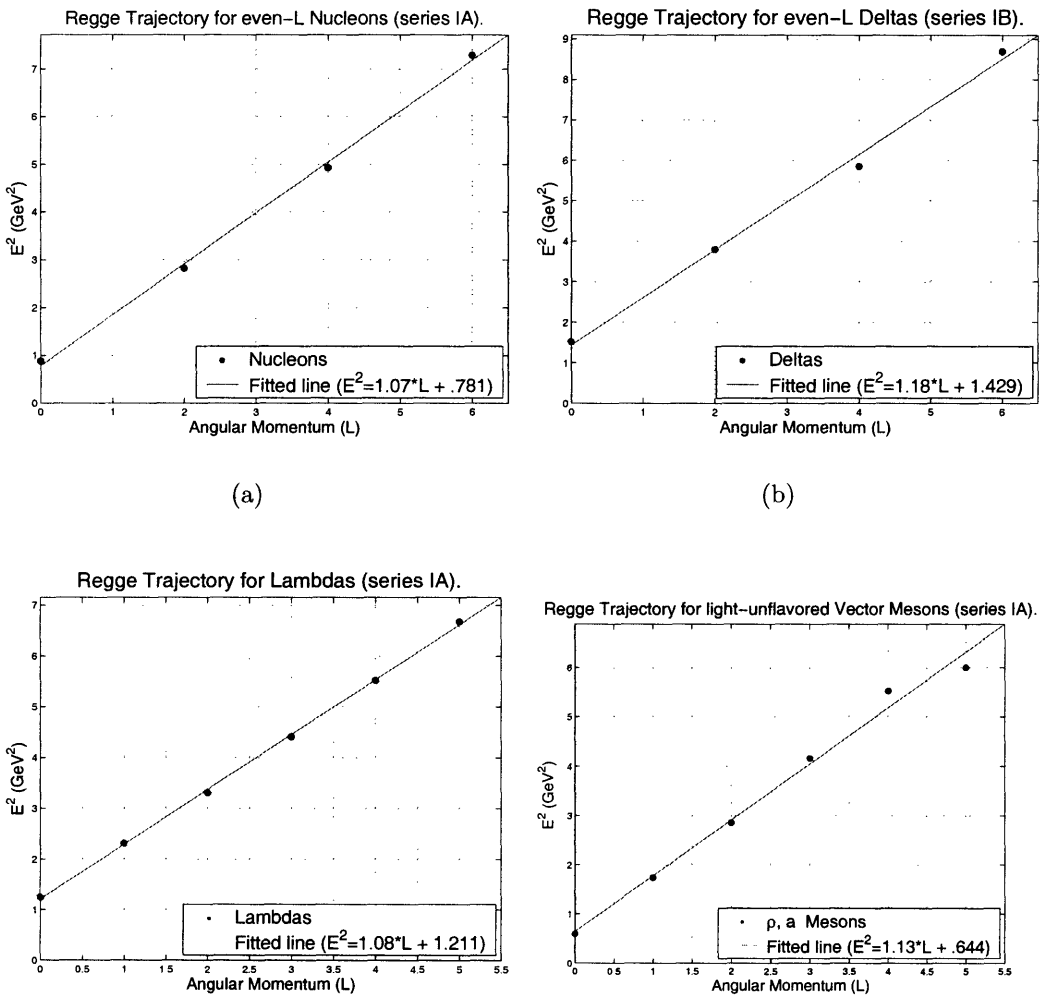


Figure 3-5: Plots of the most prominent Regge trajectories.

Table 3.3: These are the fitted parameters as before, but only with series containing three or more points. The average $\sigma$ based on these is 1.18 GeV$^2$, with standard deviation .149.

| Sector | Series | points in series | $\sigma$ (GeV$^2$) | $a$ (GeV$^2$) |
|---|---|---|---|---|
| nucleons | IA. even | 4 | 1.07 | .781 |
| deltas | IB. even | 4 | 1.18 | 1.429 |
| lambdas | IA. | 6 | 1.08 | 1.211 |
| sigmas | IB. even | 3 | 1.15 | 1.404 |
| sigmas | IB. odd | 3 | 1.09 | 1.849 |
| cascades | IA. even | 3 | .969 | 1.779 |
| rho/a | IA. | 6 | 1.13 | .6444 |
| omega/$f$ | IB. | 5 | 1.16 | .5527 |
| phi/$f$ | IC. | 3 | 1.19 | 1.072 |
| pi/$b$ | IIa singlet | 3 | 1.39 | .0599 |
| eta | IIb singlet | 3 | 1.20 | .2574 |
| kaon | I. | 5 | 1.19 | .7962 |
| kaon | II. | 5 | 1.56 | .229 |

particularly striking, and no even-odd effect is discernible in it. This is consistent with our tunneling interpretation, since for $[ud]s$ rotation through $\pi$ can only be mimicked by triple-tunneling, which plausibly is negligible.

With these classifications in place, we might expect to find a more energetic trajectory of sigmas containing a $[ls]$ diquark and an approximately degenerate trajectory of lambdas (with the right combination of isospin, $I_3 = 0$). Experimentally, while the lambdas are not [yet] seen, there is a plausible sigma trajectory, which implies a splitting of $[ls] - [ud] \sim 100$ MeV. Presumably an $(ll)$ diquark assignment to these would produce a higher splitting, allowing us to conclude this to be the correct classification. Furthermore, according to our even-odd effect hypothesis, such a series contains favorable tunneling conditions to produce such an effect. On a typical Regge plot, it becomes difficult to see the effect, but it certainly exists on a much smaller scale. This would indicate the tunneling amplitude here is much smaller than the purely light quark case of the nucleon-delta sector. We can see a clear signature for the effect by searching for oscillating slopes between particles of even-L and odd-L. Doing this for the slopes between $L = 0$ and 1, 1 and 2, 2 and 3, etc., we find values

Table 3.4: Lambda-Sigma Classifications

**I. Maximal spin alignment for "Good" and "bad" diquarks.**

| *Angular Mom. (L)* | **A. [ud]—s** ——↑ | **B. [ls]—l** ——↑ | **C. (ls)—l** ⇑—↑ |
|---|---|---|---|
| 0 | $\Lambda(1116)\ 1/2^+$ | $\Sigma(1193)\ 1/2^+$ | $\Sigma(1385)\ 3/2^+$ |
| 1 | $\Lambda(1520)\ 3/2^-$ | $\Sigma(1670)\ 3/2^-$ $\Lambda(1690)\ 3/2^-$ | $\Sigma(1775)\ 5/2^-$ $\Lambda(1830)\ 5/2^-$ |
| 2 | $\Lambda(1820)\ 5/2^+$ | $\Sigma(1915)\ 5/2^+$ | $\Sigma(2030)\ 7/2^+$ |
| 3 | $\Lambda(2100)\ 7/2^-$ | $\Sigma(2250)\ ?^?$ | |
| 4 | $\Lambda(2350)\ 9/2^+$ | $\Sigma(2455)\ ?^?$ | |
| 5 | $\Lambda(2585)\ ?^?$ | $\Sigma(2620)\ ?^?$ | |

**IIa. One "unit" less than maximal alignment.**

| *Angular Momentum (L)* | **A. [ud]—s** ——↓ | **B. [ls]—l** ——↓ | **C. (ls)—l** ⇑—↓ or ⇔—↑ |
|---|---|---|---|
| 1 | $\Lambda(1405)\ 1/2^-$ | $\Sigma(1620)\ 1/2^-$ $\Lambda(1670)\ 1/2^-$ $\Sigma(1690)\ ?^?$ | NONE |
| 2 | | $\Lambda(1890)\ 3/2^+$ | |

**IIb. One "unit" less than maximal alignment, (cont'd).**

| *Angular Momentum (L)* | **A. (ls)—l** ⇓—↑ or ⇔—↓ |
|---|---|
| 1 | $\Sigma(1750)\ 1/2^-$ $\Lambda(1800)\ 1/2^-$ |
| 2 | $\Sigma(2080)\ 3/2^+$ |

of 1.36, .878, 1.39, .964, and .837 GeV$^2$ respectively, all of which, with the exception of the last one follow the desired pattern. As such we predict that mass estimates for the the $\Sigma(2620)$ (the last resonance of this series) are too low should it be found with $J^P = \frac{11}{2}^-$. As a check, undertaking the same analysis between all points in the $\Lambda$ series IA, we find a completely constant slope as expected.

Finally we examine the bad diquark members of this series (with $(ll)$), expecting both lambdas and sigmas depending on their isospin. There are three appropriate $\Sigma$ candidates for $L = 0, 1, 2$ and one $\Lambda$ for $L = 1$ (note that the $\Lambda$ configuration is forbidden by Fermi statistics for $L = 0$, assuming a common spatial wave function). The $\Sigma$s could support either $(ll)$ or $(ls)$ diquarks; the observed eigenstates are presumably a mixture. The $\Lambda(1830)\ \frac{5}{2}^-$ is fully 55 MeV heavier than its $\Sigma(1775)\ \frac{5}{2}^-$ "partner", and 310 MeV heavier than the good-diquark $\Lambda(1520)\ \frac{3}{2}^-$. These splittings are a bit larger than others of the same kind we see elsewhere. As expected, there is also an indication of an even-odd effect here. Indeed, $\sqrt{\frac{1}{2}(1385^2 + 2030^2)} = 1738 < 1775$. Also looking the slope between $\Sigma(1385)$ and $\Sigma(1775)$ we find a value of 1.23 GeV$^2$, while between $\Sigma(1775)$ and $\Sigma(2030)$ a lower one of .97 GeV$^2$ as expected.

The second and third series are more sparsely represented (the fourth is not even seen), and they present some challenging puzzles. The $\Lambda(1405)\ \frac{1}{2}^-$ is surprisingly light and it has been suggested that its mass may be perturbed by the nearby $NK$ threshold [2]. Also the absence of a good candidate for the $\Lambda$ state corresponding to good-diquark $[ud]s$ for $L = 2$, while $[us]d$ has one, is also surprising. Finally there are two 2* $\Sigma$ resonances in the mass region where we expect the $L = 1, J^P = \frac{1}{2}^-$, namely $\Lambda(1620)\ \frac{1}{2}^-$ and $\Lambda(1690)\ ?^?$. Ideally these should be represented as the same state with some intermediate mass [2]. Finally, the complete absence of representatives of the bad diquark configurations $(ls)l$ in the second series, while appearing in the first series and third, lead one to predict the existence of $\Sigma(1760)\ \frac{3}{2}^-$, $\Sigma(2055)\ \frac{5}{2}^+$, $\Lambda(1815)\ \frac{3}{2}^-$, to fill in the holes. (All these masses should be taken $\pm 50$ MeV.) [2]

Nevertheless, in good agreement with hypothesis 6′ we have approximate degeneracies: $\Sigma(1670)\ \frac{3}{2}^-$, $\Lambda(1690)\ \frac{3}{2}^-$, $\Lambda(1670)\ \frac{1}{2}^-$, $\Sigma(1620-1690?)\ \frac{1}{2}^-$; $\Sigma(1915)\ \frac{5}{2}^+$, $\Lambda(1890)\ \frac{3}{2}^+$; and $\Sigma(1775)\ \frac{5}{2}^-$, $\Lambda(1830)\ \frac{5}{2}^-$- $\Sigma(1750)\frac{1}{2}^-$-$\Lambda(1800)\frac{1}{2}^-$, $\Sigma(2030)\frac{7}{2}^+$-$\Sigma(2080)\frac{3}{2}^+$. Also

Table 3.5: Cascades and Omega Classifications

**I. Maximal spin alignment for "Good" and "bad" diquarks.**

| *Angular Momentum (L)* | **A. [ls]—s** —⟶ | **B. (ls)—s** ⇑—⟶ | **C. (ss)—s** ⇑—⟶ |
|---|---|---|---|
| 0 | $\Xi(1318)\ 1/2^+$ | $\Xi(1530)\ 3/2^+$ | $\Omega(1672)\ 3/2^+$ |
| 1 | $\Xi(1690)\ ?^?$ | | |
| 2 | $\Xi(1950)\ ?^?$ | | |
| 3 | $\Xi(2250)\ ?^?$ | | |
| 4 | $\Xi(2370)\ ?^?$ | | |

**II. "Bad" diquarks with net spin 1/2 aligned**

| *Angular Momentum (L)* | **A. (ls)—s** ⇑—⟵ or ⇔—⟶ |
|---|---|
| 1 | $\Xi(1820)\ 3/2^-$ |
| 2 | $\Xi(2030)\ ?^?$ |

as seen in Table 3.2, the slopes are consistent with the universal value.

The data on cascades is also sparse, especially in regard to spin-parity assignments, so that the classification are necessarily assumptive (see Table 3.5). Should these correct assignments, then it is noteworthy to mention that here too one finds oscillating slopes, especially in series IA, as expected from the tunneling of the $l$ quark. We also find a lower than usual slope between $\Xi(1820)$ and $\Xi(2030)$–all in agreement with the even-odd effect. The omega sector data is worse, to the point where nothing interesting can be said.

## 3.3 The Light Mesons

The classification of the mesons do not require any novel ideas with regard to the previous literature–there are no diquarks, and the string model is as old as the field itself. Nevertheless drawing the analogy of the mesons to the diquark model of baryons, it is

Table 3.6: Light Unflavored Mesons. The PDG convention of $J^{PC}$ is used.

**I. Maximal spin alignment**

| *Angular Momentum (L)* | All with spin $\Uparrow$ | | |
|---|---|---|---|
| | **A. $I = 1$** | **B. $I = 0$, no $s\bar{s}$** | **C. $s\bar{s}$** |
| 0 | $\rho(770)\ 1^{--}$ | $\omega(783)\ 1^{--}$ | $\phi(1020)\ 1^{--}$ |
| 1 | $a(1320)\ 2^{++}$ | $f(1270)\ 2^{++}$ | $f'(1525)\ 2^{++}$ |
| 2 | $\rho(1690)\ 3^{--}$ | $\omega(1670)\ 3^{--}$ | $\phi(1850)\ 3^{--}$ |
| 3 | $a(2040)\ 4^{++}$ | $f(2050)\ 4^{++}$ | |
| 4 | $\rho(2350)\ 5^{--}$ | | |
| 5 | $a(2450)\ 6^{++}$ | $f(2510)\ 6^{++}$ | |

**IIa. Neutral spin orientation, with $I = 1$**

| *Angular Momentum (L)* | spin triplet $\Leftrightarrow$ | spin singlet $-$ |
|---|---|---|
| 0 | | $\pi(140)\ 0^{-+}$ |
| 1 | $a(1260)\ 1^{++}$ | $b(1235)\ 1^{+-}$ |
| 2 | | $\pi(1670)\ 2^{-+}$ |

**IIb. Neutral spin orientation, with $I = 0$**

| *Angular Momentum (L)* | **A. with no $s\bar{s}$** | | **B. $s\bar{s}$** | |
|---|---|---|---|---|
| | $\Leftrightarrow$ | $-$ | $\Leftrightarrow$ | $-$ |
| 0 | | $\eta(550)\ 0^{-+}$ | | $\eta'(960)\ 0^{-+}$ |
| 1 | $f(1285)\ 1^{++}$ | $\eta(1170)\ 1^{+-}$ | $f(1420)\ 1^{++}$ | $\eta'(1380)\ 1^{+-}$ |
| 2 | | $\eta(1645)\ 2^{-+}$ | | |

**III. Maximal spin anti-alignment**

| *Angular Momentum (L)* | All with spin $\Downarrow$ | | |
|---|---|---|---|
| | **A. $I = 1$** | **B. $I = 0$, with no $s\bar{s}$** | **C. $s\bar{s}$** |
| 1 | $a(1450)\ 0^{++}$ | $f(1370)\ 0^{++}$ | $f(1500)\ 0^{++}$ |
| 2 | $\rho(1700)\ 1^{--}$ | $\omega(1650)\ 1^{--}$ | $\phi(1680)\ 1^{--}$ |
| 3 | | $f(2010)\ 2^{++}$ | $f(2300)\ 2^{++}$ or $f(2340)\ 2^{++}$ |

Table 3.7: Light Strange Mesons ($S = \pm 1$)

| *Angular Mom.* ($L$) | **I. Spin aligned** $\Uparrow$ | **II. Spin neutral** $\Leftrightarrow$ **or** $-$ | **III. Spin anti-aligned** $\Downarrow$ |
|---|---|---|---|
| 0 | $K^*(892)\ 1^-$ | $K(495)\ 0^-$ | - |
| 1 | $K^*(1430)\ 2^+$ | $K(1270)\ 1^+$ $K(1400)\ 1^+$ | $K^*(1430)\ 0^+$ |
| 2 | $K^*(1780)\ 3^-$ | $K(1770)\ 2^-$ $K(1820)\ 2^-$ | $K^*(1680)\ 1^-$ |
| 3 | $K^*(2045)\ 4^+$ | $K(2320)\ 3^+$ | |
| 4 | $K^*(2380)\ 5^-$ | $K(2500)\ 4^-$ | |

instructive to classify and fit the meson series to Regge trajectories to compare their slopes and for possible calculations in comparing quark masses to diquarks masses. As such, our classification of the light mesons (those classified with a dot in the PDG) are listed in Tables 3.6 and 3.7, while their Regge fit values are given in Table 3.2.

In particular this program yields consistent slopes with the baryons, supporting the idea of the diquark as effectively having the color of an antiquark. There are also approximate degeneracies for states with the same $L$ but different spin alignment, and in several cases we have approximately degenerate particles corresponding to a vector meson neutrally aligned versus a singlet.

The $\pi(140)$ is not surprisingly a little anomalous, and it causes the trajectory to have a small intercept and higher than usual slope (entry pi/$b$ in Table 3.2). However this $L = 0$ may well be described in another language, as an approximate Nambu-Goldstone boson [2].

## 3.4 Exceptional Cases

There were several particles that were not classified. In the traditional quark model these all correspond to being interpreted as having internally excited quarks or in some cases the particles defy classification. The diquark system presents no inconsistencies with any of the traditional views. It does, however, offer the possibility of some new interpretations. Nevertheless, to give a better treatment of these ideas, it is necessary to have a better understanding of effective diquark masses and mass parameters

entering into the flux tube ends of the model. As such, we shall postpone these discussions until the following chapter. For completeness I shall list the particles that have been left out; in the baryon sector: $N(1440)\ \frac{1}{2}^+$, $N(1710)\ \frac{1}{2}^+$, $\Delta(1600)\ \frac{3}{2}^+$, $\Delta(1930)\ \frac{5}{2}^-$, $\Delta(1900)\ \frac{1}{2}^-$, $\Lambda(1600)\ \frac{1}{2}^+$, $\Lambda(2110)\ \frac{5}{2}^+$, $\Sigma(1660)\ \frac{1}{2}^+$, and $\Sigma(1940)\ \frac{3}{2}^-$; and in the meson sector: $f(1710)\ 0^{++}$, $f(2300)\ 2^{++}$ (or $f(2340)\ 2^{++}$), $f(600)\ 0^{++}$, $a(980)\ 0^{++}$, $\rho(1450)\ 1^{--}$, $f(980)\ 0^{++}$, $\omega(1420)\ 1^{--}$, $\pi(1300)\ 0^{-+}$, $\pi(1800)\ 0^{-+}$, $\eta(1295)\ 0^{-+}$, and $\eta(1440)\ 0^{-+}$.

## 3.5 Heavy Quark Hadrons

The framework we have been using for the classification and fits of all hadrons and exotics containing "light" quarks, can also be successfully extended to those containing heavy quarks. Because the spectrum for particles containing more than one heavy quark/antiquark is quite limited, I will consider only resonances that have just one heavy quark/antiquark, paired with other light quarks.

In these cases, then, we have a heavy and a light end which conveniently fits the prescription used to derive equation 2.15. Hence we might expect that these resonances can be fit by the expression

$$(E - M_Q)^2 = \frac{\sigma}{2}L + a, \tag{3.3}$$

where $\sigma$ is of course the slope associated with the massless string ($2\pi T$), or the fits of light quark hadrons, and $M_Q$ is the mass of the heavy quark. The intercept $a$, has possible interpretations as previously discussed.

With regard to the baryons it's only worthwhile to talk about the charmed lambdas and sigmas. Table 3.8 summarizes the classifications of all existing charmed lambda/sigma resonances. The most "prominent" series is IA, which has three resonances – the minimum required to obtain a fit for our model given by equation 3.3. If we do so, we obtain values of: $\sigma = 1.212\ \text{GeV}^2$, $M_Q = 1.562\ \text{GeV}$, and $a = .522\ \text{GeV}^2$. In particular the slope and $M_Q = M_c$ the mass of the charm quark is well within the

Table 3.8: Charmed Lambda-Sigma Classifications

| **I. Maximal spin alignment for "Good" and "bad" diquarks.** | | |
|---|---|---|
| *Angular Momentum (L)* | **A. [ud]—c** ——↑ | **B. (ll)—c** ⇑—↑ |
| 0 | $\Lambda_c(2285)\ 1/2^+$ | $\Sigma_c(2520)\ 3/2^+$ |
| 1 | $\Lambda_c(2625)\ 3/2^-$ | |
| 2 | $\Lambda_c(2880)\ 5/2^+$ | |
| **II. One "unit" less aligned.** | | |
| *Angular Momentum (L)* | **A. [ud]—c** ——↓ | **B. (ll)—c** ⇑—↓ or ⇔—↑ |
| 0 | - | $\Sigma_c(2455)\ 1/2^+$ |
| 1 | $\Lambda_c(2593)\ 1/2^-$ | $\Sigma_c(2750)\ 3/2^-$ |

expected range. Furthermore, if we recall that even at low $L$ the real relation of $E^2$ vs $L$ has a slightly higher slope than our approximated model (see Figure A in the appendix), it helps to explain why the slope is higher than usual.

Finally while the other series do not have enough points for a complete fit, if we take the fitted mass of the charm quark, we can extract $\sigma$ of series IIB to be 1.228 $\text{GeV}^2$ – also in agreement.

The heavy meson trajectories are even more sparse. They are classified in table 3.9. As before, using the only fitted mass for the charm quark that we have, we can get the slopes of the various meson series. Specifically for series IA, IIA, and IIB we get $\sigma$'s of 1.216, 1.290, and 1.438[1] respectively. Again these are slightly higher than the slopes of the light-quark-containing hadrons. What is remarkable is the consistency between cases, with the exception of the meson series IIB, whose higher value might be explained by an unusually low mass for the scaler $D$ and because we should expect more deviation from the approximation of equation 2.15 due to the larger strange quark mass.

[1]The average of the scaler and vector $D$'s was used.

Table 3.9: Heavy Quark Mesons For all the columns in series II, there are another two particles to be expected due to the two spin possibilities listed. There are no particles with spins antialigned.

| **I. Maximal spin alignment** | | | |
|---|---|---|---|
| *Angular* | All with spin ⇑ | | |
| *Mom.* ($L$) | **A. cl** | **B. c$\bar{s}$** | **C. bl** |
| 0 | $D^*(2007)^0$ $1^-$ | $D^*(2111)$ $?^?$ | $B^*(5325)$ $1^-$ |
| | $D^*(2010)^\pm$ $1^-$ | | |
| 1 | $D^*(2460)^0$ $2^+$ | $D_s^*(2573)^\pm$ $?^?$ | |
| | $D^*(2460)^+$ $2^+$ | | |

| **II. Neutral spin alignment** | | | |
|---|---|---|---|
| *Angular* | Spin triplet ($\Leftrightarrow$) or singlet ($-$) | | |
| *Mom.* ($L$) | **A. cl** | **B. c$\bar{s}$** | **C. bl** |
| 0 | $D(1864)^0$ $0^-$ | $D_s(1971)^\pm$ $0^-$ | $B(5279)^0$ $0^-$ |
| | $D(1869)^\pm$ $0^-$ | | $B(5279)^\pm$ $0^-$ |
| 1 | $D(2420)^0$ $1^+$ | $D(2536)^\pm$ $1^+$ | |

### 3.5.1 Application to Exotics

The validated heavy-light end mass formula (at least for low $L$), can naturally be used for exotics containing a heavy quark. In light of this, the recent exotic ($B = 1$, $c = -1$) observed at 3099 MeV [33] has a natural interpretation. Specifically it has a structure of $[ud]\bar{c}$—$[ud]$, and as such we'll refer to it as $\Theta_c$ [34, 35, 36]. Applying our mass formula, we have the relation:

$$(E - M_c)^2 = \frac{\sigma_h}{2} L + (\delta m)^2 \tag{3.4}$$

where $E$ is the mass of a $\Theta_c$ for a particular $L$, $\sigma_h$ is a typical slope for the heavy-quark hadrons which is slightly higher than the usual $\sigma$ due to the approximation error (about 1.2 GeV$^2$), and $\delta m$ would be a mass characteristic of what remains if we "remove" the charm quark contribution at $L = 0$. Thus possible candidates for $\delta m$ would be something of the mass of the roper $N(1440)$ or the $\Theta_s(1530)$ but at

$L = 0$, since these are quoted masses for $L = 1$ particles. As the roper may be the better of two, we find using equation 2.2 that $(\delta m)^2 = M^2_{roper} - \sigma$. Plugging this into equation 3.4 and rearranging gives the following mass formula:

$$E = Mass[\Theta_c(L)] = \sqrt{\frac{\sigma_h}{2}L + M^2_{roper} - \sigma} + M_c. \tag{3.5}$$

Using the previously fitted values $M_c = 1.562$, $M_{roper} = 1.440$ GeV, and characteristic $\sigma = 1.1$, $\sigma_h = 1.25$ GeV$^2$, we get the mass of $\Theta_c$ with $L = 1$ $J^P = \frac{1}{2}^+$ (spin 1/2 antialigned as corresponding to the roper) to be 2826 MeV; $\Theta_c$ with $L = 2$ $J^P = \frac{3}{2}^-$ at 3053 MeV; and $\Theta_c$ with $L = 3$ $J^P = \frac{5}{2}^+$ at 3250 MeV. This identifies the observed particle as a $\Theta_c$ with $L = 2$, $J^P = \frac{3}{2}^-$. Furthermore, one might reason that our result has a smaller than expected mass because we have not taken into account the effect of the diquark on the heavy-end mass so that something more than the mass of just $M_c$ should be used; as the end is not just a charm antiquark but a charm antiquark paired with the $[ud]$ diquark.

## 3.6 Even-Odd Effect and Tunneling

The tunneling hypothesis to explain the even-odd effect can be used to estimate the overlap between a given quark-diquark configuration and its tunneled state–the configuration rotated by $\pi$. In non-relativistic quantum mechanics, we could then know the tunneling amplitude. In the context of non-relativistic quantum mechanics such an amplitude would also be related to the potential barrier between the ends of the particle. Presumably the overlap would also be related to the physical separation of the flux-tube ends, thus giving one a rough idea as to the separation of the ends. For these reasons, it would be instructive even if crude, to know the overlap and non-relativistic tunneling amplitude, from the energy difference in even versus odd $L$.

To begin to address the problem, we define $|a\rangle$ to be the wave function of a particular quark-diquark configuration. Similarly we let $|b\rangle$ the wave function of the same configuration, but rotated by $\pi$. That is, $|b\rangle = P|a\rangle$, where $P$ is the parity

operator. In general we will take $\langle b|a\rangle \neq 0$, and furthermore, given the definition of $|a\rangle$ and $|b\rangle$, $\langle b|a\rangle = \langle a|b\rangle$. As mentioned, because of tunneling, presumably the true particle wave function, $\Psi_L$ is some linear combination of these:

$$\Psi_L = \alpha\,|a\rangle + \beta\,|b\rangle\,, \tag{3.6}$$

with the condition that, $P\Psi_L = (-1)^L\Psi_L$. When this condition is enforced, we obtain the general and expected expression:

$$\Psi_L = N_L(|a\rangle + (-1)^L\,|b\rangle), \tag{3.7}$$

with $N_L^2 = \frac{1}{2(1+(-1)^L\langle b|a\rangle)}$. Our goal then is to relate the overlap $\langle b|a\rangle$ to the energies of the odd and even $L$ states.

By definition we shall assume some Hamiltonian, $H$, acts on our state such that:

$$H\Psi_L = E_L^+\Psi_L, \quad for\ odd\ L \tag{3.8}$$

$$H\Psi_L = E_L^-\Psi_L, \quad for\ even\ L, \tag{3.9}$$

with the understanding that $E^+ > E^-$ (the $+/-$ here is associated with higher or less energy not parity). Also, from now on we make the $L$ dependence implicit dropping all $L$ subscripts, while letting $\Psi_L \to \Psi_{even}, \Psi_{odd}$ and $N_L \to N_{even}, N_{odd}$ depending on even or odd $L$ respectively. To make progress then, we might crudely approximate the even-odd effect by treating the Hamiltonian as having some typical $L$-dependent part which I'll call $H_o$, and some even-odd splitting term, $-kP$, where $k$ is some positive constant and $P$ is the parity operator (the negative sign enters because odd $L$ states, which have negative parity, are higher in energy). Furthermore we take $H_o\Psi_{even,odd} = E_o\Psi_{even,odd}$. Then we have:

$$\begin{aligned} H\Psi_{even} &= E^-\Psi_{even} = (E_o - k)\Psi_{even} \\ H\Psi_{odd} &= E^+\Psi_{odd}, = (E_o + k)\Psi_{odd} \end{aligned} \tag{3.10}$$

where the second equality is the explicit calculation by decomposing $H$. Setting the respective energies equal, and solving, we obtain the relations:

$$k = \frac{E^+ - E^-}{2}, \qquad E_o = \frac{E^+ + E^-}{2}. \tag{3.11}$$

Now what can we say about the eigenvalues $E^+$, $E^-$ in terms of the overlap $\langle b|a\rangle$? We consider the overlaps of $H$ in the $|a\rangle$, $|b\rangle$ (non-orthogonal) basis. In particular, by symmetry $\langle a| H |a\rangle = \langle b| H |b\rangle$ and $\langle b| H |a\rangle = \langle a| H |b\rangle$. And using the assumptions about $H$ given above we can explicitly calculate $\langle b| H |a\rangle$. We have:

$$\begin{aligned} \langle b| H |a\rangle &= \langle b| H \left( \frac{\Psi_{even}}{N_{even}} - |b\rangle \right) \\ &= E^- \langle b| (|a\rangle + |b\rangle) - \langle b| H |b\rangle \\ &= E^-(\langle b|a\rangle + 1) - \langle b| H |b\rangle . \end{aligned} \tag{3.12}$$

A similar calculation for the odd state gives:

$$\langle b| H |a\rangle = E^+(\langle b|a\rangle - 1) + \langle b| H |b\rangle . \tag{3.13}$$

Subtracting these, and after some algebra, we obtain:

$$\langle b|a\rangle = \frac{E^+ + E^- - 2\langle b| H |b\rangle}{E^+ - E^-} = \frac{E^+ + E^- - 2\langle a| H |a\rangle}{E^+ - E^-}. \tag{3.14}$$

With what has been thus assumed nothing further can be said. However, we might try to estimate the value of $\langle a| H |a\rangle$ as a function of $L$ (for a given trajectory we know $E^-$ and $E^+$ as functions of $L$). First we note that in the absence of tunneling, or at large $L$, this term should approach $E_o$, while at small $L$ with full overlap, this term approaches $E^-$. If we knew the isolated masses at a string end (along with the tension), then we might crudely estimate this value by simply calculating the Chew-Frautschi trajectory (expression 2.10) for the given isolated masses. To get an idea of how the amplitude falls, we might do this for the nucleon and delta sectors using effective values .141 and .271, .517 (GeV) for the quark and good and bad diquarks,

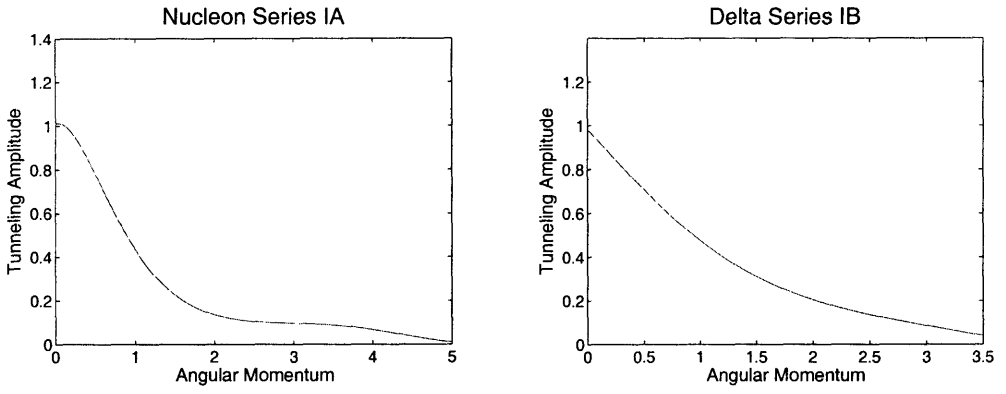


(a) (b)

Figure 3-6: Approximate measures of the tunneling amplitudes, $|\langle b|a\rangle|^2$, for the sectors where the even-odd effect is most prominent.

respectively, that will be calculated in the following chapter. In practice, we need to make certain approximations of the general expressions by transforming them into polynomials and matching the asymptotic cases. As such the results are very crude but illustrative. These are plotted in Figure 3.6 for the nucleon and delta series IA and IB respectively.

Note that we have reason to doubt $L > 4$ values in the delta trajectory, because the odd trajectory has dubious values as its slope coming from just two points (the odd and even trajectories will cross with the given values). Nevertheless, this simple program captures two salient characteristics. First we note that the bad diquark generally have higher tunneling amplitude, as expected. But most importantly, there seems to be a large barrier for tunneling as the amplitude rapidly becomes small. Hence whether the quark and diquark are well separated at small $L$, is perhaps not as relevant as previously thought, if there is a large barrier between them. This is consistent with the paradox that the degrees of freedom between the string ends are fairly independent, while the ends might remain in proximity.

# Chapter 4

# Diquark Masses and Applications to Cryptoexotic States

An interesting prospect which the classification of the particles immediately suggests is the possibility of determining *effective* diquark masses, or at least mass differences.

As already suggested differences between diquarks can be estimated by looking at the energy differences between particles in different trajectories, like in the nucleon sector. A little more precise approach, might involve comparing ground states energies of particles containing a single heavy quark, where in such particles a diquark can safely be presumed to exist even at $L = 0$. Doing these "comparisons" by taking mass differences for various $(Qqq)$ baryons and $(Q\bar{q})$ mesons, one can extract diquark mass differences as well as differences between diquarks and quarks. In doing such comparisons, spin-spin forces have to be taken into account, and proper linear combinations between vector symmetric states and antisymmetric states have to be taken. These calculations have been performed by Jaffe [27], and we shall simply quote the results here. Using the the notation $\mathcal{D}|_Q$ meaning the mass of $\mathcal{D}$ using $Q$ as the "spectator

quark", the results were:

$$
\begin{aligned}
(ud)|_s - [ud]|_s &= 205\,\text{MeV} \\
(ud)|_c - [ud]|_c &= 212\,\text{MeV} \\
\\
[ud]|_s - u|_s &= 321\,\text{MeV} \\
[ud]|_c - u|_c &= 312\,\text{MeV} \\
[ud]|_b - u|_b &= 310\,\text{MeV} \\
\\
(us)|_c - [us]|_c &= 152\,\text{MeV} \\
\\
[us]|_c - s|_c &= 498\,\text{MeV}\,.
\end{aligned}
\tag{4.1}
$$

As was pointed out by Jaffe, these imply a consistency in the diquark differences regardless of the spectator quark used, and furthermore the original intuition of $(ud) - [ud] > (us) - [us]$, is in agreement (see chapter 2 section 2.1).

However, knowing how the masses enter into the expression for the energy of the relativistic rotating string (see chapter 2 section 2.4.1), we could use the whole of the experimental data to extract effective masses. In particular there are two main programs one can undertake, inherently related to the problem of interpreting the intercept of the Regge fit. The reader might recall the discussion presented in chapter 2 section 2.4. The first view, makes no reference to a quantum mechanical source of ground state angular momentum, and simply adheres to a semi-classical relativistic string with some effective masses accounting for the trajectory as it is seen. While the second view, postulates an inherent ground state angular momentum modifying the intercept. In what follows, I shall use each of these interpretations to extract effective masses.

I'll begin with the interpretation that assumes no explanation for a Regge intercept other than effective masses. The calculated Regge trajectory for such a string with

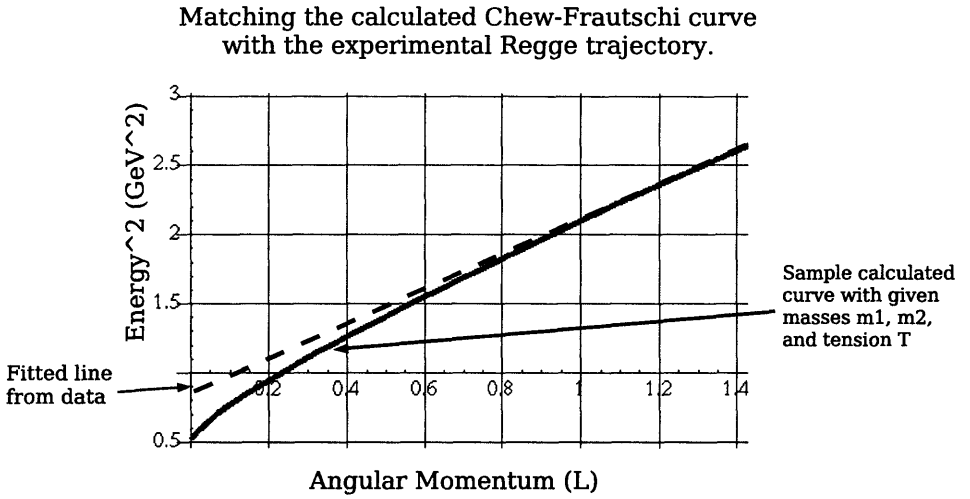


Figure 4-1: We can use the experimentally fitted Regge trajectory to select masses $m_1$, $m_2$, using the tension/slope of the line, that will match it above $L = 1$ as shown.

heavy masses will presumably have some nonlinearity at the small $L$ which is absent experimentally (see plots in appendix A). Thus we are forced to assume, that some other interactions come into play to correct the nonlinearity and keep the trajectory linear. Still we might ask, what masses $m_1$ and $m_2$, given a string tension, are needed so that the theoretical trajectory matches the experimental line. This idea is shown in figure 4-1. Undertaking this procedure, we can calculate the actual values of masses $m_1$ and $m_2$ for a given trajectory. In general we cannot solve for the simultaneous values of $m_1$ and $m_2$ that will satisfy this matching, but we might begin with meson trajectories having equivalent ends to solve for one mass. In general we can proceed as follows:

1. Determine the effective $u/d$ mass from the pion, eta, rho, and omega trajectories (proper linear combinations should be taken to eliminate spin-spin interaction;

this will be elaborated upon below).

2. Determine the effective $s$ mass purely from the phi/$f$ series IC, or by using the calculated $u/d$ mass and inserting it into the kaon series.

3. Given the strange mass, determine the $[ud]$ mass from the lambda series IA, or given the $u/d$ mass from the nucleon series IA.

4. Similarly for the $[us]$, from sigma IB or cascades IA.

5. Determine the $(ud)$ using the quark masses and by taking linear combinations of the delta trajectories (given $u/d$ mass).

6. Determine the $(us)$ using the quark masses and by taking linear combinations of the sigma trajectories (given $u/d$ mass).

As noted in Ref. [27], for vector mesons and bad diquarks, spin-spin interactions may affect the energies, and therefore linear combinations must be taken. In particular assuming an interaction of the form $\sim s_1 \cdot s_2$, then for a $(s_1+s_2) = \frac{3}{2}$ baryon, $B^*$, and a $(s_1+s_2) = \frac{1}{2}$ baryon, $B$, the proper combination is $(2B^*+B)/3$. Similarly for vector and singlet mesons, $M^*$, $M$ respectively, the combination should be $(3M^* + M)/4$. In the context of Regge Trajectories, we will approximate the superposition of two trajectories, as superpositions of the slope and intercept, that is, for constants $\alpha$, $\beta$,

$$\left(\frac{\alpha}{\alpha+\beta}\sqrt{\sigma_1 L + a_1} + \frac{\beta}{\alpha+\beta}\sqrt{\sigma_2 L + a_2}\right)^2 \approx \frac{\alpha(\sigma_1 L + a_1) + \beta(\sigma_2 L + a_2)}{\alpha+\beta}, \qquad (4.2)$$

which holds given the validity of hypothesis 6′ or when the trajectories do not defer in value too much. Also in the nucleon-delta sectors where the even-odd effect can be substantial, a simple average is taken between these two trajectories. In other cases, where the data is scarce and the effect is much less important, it is ignored.

The masses calculated by carrying through these procedures are given table 4.1. The various differences taken in the table serve as comparison to some of the previous values. Values with the asterisks come from scarce and questionable trajectories, some with only two points. However the bad good $ll$ diquark difference is fairly

Table 4.1: Calculated effective masses. The "obtained values" column has the different results when more than one method can be used as explained in the text. When the mass of any object is calculated given another, the average or "approximate final value" is used as input. For the bad diquarks, the asterisks indicate scarce trajectories, and therefore very uncertain values.

| | Approx. Final Value (MeV) | Obtained Values; Remarks |
|---|---|---|
| $u/d$ | 141 | (linear combin. of $\eta$-$\pi$ and $\rho$-$\omega$ averaged from the onset) |
| $s$ | 210 | 191, from $K$s, given $u/d$; 237, from $\phi/f$'s |
| $[ud]$ | 271 | 321 from $\Lambda$s, given $s$; 221, from $N$s given $u/d$ |
| $[us]$ | 479 | 467, from $\Sigma$s, given $u/d$; 490, from $\Xi$s, given $s$ |
| $(ud)$ | 517* | 623, from linear combin. of $\Delta$-IBeven with average of $N$-IIBodd, $\Delta$-IIBeven; 411, with only $\Delta$-ICeven (given $u/d$) |
| $(us)$ | 517* | (from $\Sigma$ IC-even and IIbA given $u/d$) |
| $[ud]-2u/d$ | -11 | |
| $[us]-u-s$ | 128 | |
| $[us]-[ud]$ | 208 | |
| $(ud)-[us]$ | 38* | |
| $(ud)-[ud]$ | 246* | |
| $(us)-[us]$ | 38* | |

consistent. Also note that given the absolute values of the objects, we can make the meaningful comparison of the effective mass of a diquark compared with the mass of its constituents. This suggests the favorableness for the formation of the good $[ud]$, while any extra energy associated with forming the $[us]$ is quickly overcome by $L = 1$.

Yet as mentioned, a second method to determine rough mass estimates might assume some universal intercept, thereby giving presumably smaller absolute mass values, and preserving linearity of the Regge trajectory down to $L = 0$. Then a more holistic approach can be taken by combining all particles from various baryon and meson sectors, and doing a least squares fit for the various masses and string tension to best fit this data. The universal intercept might be interpreted in the form of some inherent angular momentum. Taking this approach, an intercept of $a'$ would enter into the Regge trajectory as $\sigma a'$.

In practice, however, several prominent trajectories stand out as being most accurate and consistent. In particular these are: the nucleon IA-even, delta IB-even, lambda IA, sigma IB, kaon IA, kaon IB, rho IA, and omega IB series. From these

Table 4.2: The various fitted parameters; with the exception of the "intercept" representing an inherent ground state angular momentum that was not fitted but set at specific values (in units of angular momentum). All tension values are in $GeV^2$ and masses in MeV. The names "anchoring data" and "full data" are described in the text. Parameters labeled as "set" were not fitted, but are the values taken from the anchoring data fit. "$R_{adj}$" is the usual adjusted $R^2$ of the fit.

| Parameters | From "Anchoring Data" | | | | "Full Data" | |
|---|---|---|---|---|---|---|
| | | | | | All values set | $T$ and Int. set |
| Intercept | $\frac{1}{2}$ | $\frac{1}{3}$ | $\frac{1}{4}$ | 0 | $\frac{1}{2}$(set) | $\frac{1}{2}$(set) |
| Tension/ | .1739 | .1667 | .1625 | .1396 | .1739(set) | .1739(set) |
| Slope | 1.093 | 1.047 | 1.021 | .8771 | 1.093(set) | 1.093(set) |
| $u/d$ | 97 | 192 | 236 | 385 | 97(set) | 76 |
| $s$ | 281 | 345 | 376 | 487 | 281(set) | 221 |
| $[ud]$ | 179 | 264 | 305 | 464 | 179(set) | 223 |
| $[us]$ | 495 | 550 | 579 | 692 | 495(set) | 488 |
| $(ud)$ | 522 | 582 | 613 | 745 | 522(set) | 532 |
| $(us)$ | - | - | - | - | 729 | 753 |
| $R_{adj}$ | .977 | .976 | .976 | .966 | .960 | .966 |
| $[ud] - 2u/d$ | -14 | -121 | -166 | -305 | -14 | -15 |
| $[us] - u - s$ | 116 | 13 | -32 | -179 | 116 | 86 |
| $[us] - [ud]$ | 315 | 287 | 274 | 229 | 315 | 285 |
| $(ud) - [us]$ | 28 | 31 | 34 | 52 | 28 | 58 |
| $(ud) - [ud]$ | 343 | 318 | 308 | 281 | 343 | 343 |
| $(us) - [us]$ | - | - | - | - | 234 | 265 |

we can more accurately determine a universal tension, and the masses of the $u/d$, $s$, $[ud]$, $[us]$, and $(ud)$, for different set values of an intercept. As such I will call the data involving these series the "anchoring data". We might then use some or all of these values and add in the rest of the data, which I call the "full data" to determine the $(us)$. The results of these fits are shown in table 4.2. The "full data" involves all the previous series plus those which do not contain blatantly corrupt particles, namely: the sigma IC, cascades IA-even, cascades IB, phi/$f$ IC, eta/$f$ IIbA, eta$'$/$f$ IIbB, $a$/rho IIIA, $f$/omega IIIB, and $f$/phi IIIC series.

If we take the fitted results from the "full data" we have a fairly reasonable consistent picture with the sector by sector fit previously described and noted in table 4.1. Likewise the commentary presented there on the mass differences follow through, including the inequality that $(ud) - [ud] > (us) - [us]$. The only exception to the

consistency is the mass of the $(us)$ which is most probably wrong in the sector by sector fit as it was very crudely estimated. The overall consistency, however, is quite remarkable considering how different the methods employed were. The first method employs the slight variations in string tensions and variety of intercepts, and on average give similar results when one demands an overall intercept and universal tension. While this is discouraging with regard to distinguishing between the interpretations, we can at the same time be more certain that these effective masses are approximately valid.

## 4.1 Cryptoexotica

Having estimates of diquark masses, we are now in a position to consider multiquark states such as tetraquarks and to some extent pentaquarks, $\mathcal{D}$—$\overline{\mathcal{D}}$ and $\mathcal{D}\bar{q}$—$\mathcal{D}$ respectively (using the string/diquark notation from before). However, statements regarding pentaquarks or in particular cryptopentaquarks (5 quarks states that otherwise have the quantum numbers of baryons), are much more speculative mainly because it is difficult to estimate the favorableness and mass of the complex correlation: $\mathcal{D}\bar{q}$ which would exist at one end of the flux tube. As such we shall leave their discussion for last.

Hearkening back to the analogy of the diquark to an antiquark, a natural progression of states is suggested and expected: $(q\text{—}\bar{q}) \rightarrow (q\text{—}\mathcal{D}) \rightarrow (\overline{\mathcal{D}}\text{—}\mathcal{D})$. Of course following would be pentaquarks, but again, it is difficult to estimate the favorableness of the diquark-antiquark correlation. Nevertheless as baryons do exist, it does not seem unreasonable that replacing the quark with an antidiqaurk should be very unfavorable, especially at "large $L$". We might characterize large enough $L$, as that at which the effective energy difference between the quark and diquark becomes small, in which case tetraquarks might come into existence.

As such we might perform the calculations presented in equation 4.1 from Ref. [27], but for higher $L$ states. In particular if we do so for $L = 1$ one finds the following

| Quark Structure | | $L=1$ | $L=2$ | $L=3$ |
|---|---|---|---|---|
| $[ud]$—$[\bar{u}d]$ | A | 1329 | 1726 | 2039 |
| | B | 1480 | 1833 | 2123 |
| $[us]$—$[\bar{u}d]$ | A | 1492 | 1875 | 2178 |
| | B | 1673 | 2012 | 2293 |
| $[us]$—$[\bar{u}\bar{s}]$ | A | 1652 | 2021 | 2316 |
| | B | 1864 | 2188 | 2460 |

Table 4.3: Calculated masses (in MeV) for various tetraquark states. "A" refers to values obtain in the first interpretation where there is no inherent intercept, and "B" to the final values in table 4.2 (the second interpretation). In "A" the same tension as from "B" is used.

splittings:

$$\begin{aligned} [ud]|_{s,L=1} - u|_{s,L=1} &= 130\,\text{MeV} \\ [ud]|_{c,L=1} - u|_{c,L=1} &= 175\,\text{MeV}, \end{aligned} \tag{4.3}$$

and for $L = 2$,

$$[ud]|_{s,L=2} - u|_{s,L=2} = 27\,\text{MeV}, \tag{4.4}$$

a remarkable improvement from the ground state values. Of course, the Chew-Frautschi relation for the charm quark system at $L = 1$ shows that the system is at an effective $L = \frac{1}{2}$. As such it seems that $L = 1, 2$ is already "large enough" $L$ for possible cryptotetraquarks to appear. This may be regarded as a prediction for the existence of tetraquarks at these $L$ values.

Knowing absolute diquark masses, we might calculate the masses of these orbitally excited tetraquarks using the Chew-Frautschi relation given by equation 2.10. Of course, we have presented two possible interpretations relating to the Regge intercepts, and unfortunately each interpretation may lead to different values (especially at small $L$). As such, calculations using *both* interpretations are presented in table 4.3. These values may be regarded as predictions of the approximate masses that the tetraquarks should have.

With regard to the unclassified mesons, some states fall near these ranges, and as such they may have possible interpretations as cryptotetraquarks. However, one

Table 4.4: Speculative cryptopentaquarks and pentaquarks interpretations.

| Quark and Spin Structure | $L=1$ | $L=2$ | $L=3$ | Regge Slope |
|---|---|---|---|---|
| CRYPTOPENTAQUARKS | | | | |
| $[ud]\bar{l}$—$[ud]$, $[-]\downarrow$—$[-]$ | $N(1440)\ \frac{1}{2}^+$ | | | - |
| $[ud]\bar{l}$—$[ls]$, $[-]\downarrow$—$[-]$ | $\Lambda(1600)\ \frac{1}{2}^+$ | | $\Lambda(2110)\ \frac{5}{2}^+$ | .946 |
| | $\Sigma(1660)\ \frac{1}{2}^+$ | $\Lambda(1940)\ \frac{3}{2}^-$ | | 1.01 |
| $[ud]\bar{s}$—$[ls]$, $[-]\downarrow$—$[-]$ | $N(1710)\ \frac{1}{2}^+$ | | | - |
| $(ud)\bar{l}$—$[ls]$, Net $\frac{1}{2}$ aligned. | $\Delta(1600)\ \frac{3}{2}^+$ | $\Delta(1930)\ \frac{5}{2}^-$ | | 1.17 |
| $(ls)\bar{l}$—$[ud]$, Net $\frac{1}{2}$ anti-align. | $\Lambda(1810)\ \frac{1}{2}^+$ | | | - |
| | $\Sigma(1880)\ \frac{1}{2}^+$ | | | - |
| $(ud)\bar{l}$—$[ud]$, $[-]\downarrow$—$[\Downarrow]$ | | $\Delta(1900)\ \frac{1}{2}^-$ | | - |
| PENTAQUARKS ?, Following Ref. [34, 35, 36] | | | | |
| $[ud]\bar{s}$—$[ud]$, $[-]\downarrow$—$[-]$ | $\Theta(1530)\ \frac{1}{2}^+$ | | | - |
| $[ds]\bar{u}$—$[ds]$, $[-]\downarrow$—$[-]$ | $\Phi(1860)\ \frac{1}{2}^+$ | | | - |

would expect that such tetraquark states would have little phase space to decay into, and the small $L$ states would be too light decay into a baryon-antibaryon [2]. Presumably then, the states might be very narrow, consistent with why they may yet be undetected.

Most probably, then, the majority of unclassified mesons are possibly best explained in the traditional framework of quark excitations. The exception, are two good glueball candidates, as predicted from lattice QCD calculations [37, 38, 39]. In particular the $f(1710)\ 0^{++}$ fits well as glueball candidate as well as one of the $f(2300)$ $2^{++}$ or $f(2340)\ 2^{++}$. For a good review see non $q\bar{q}$ candidates of PDG [32].

The unclassified baryons, may also be explained in the traditional idea of internal excitation of the quarks. However, the existence of such particles like the Roper, beg the imagination for other interpretations. While much more speculative than tetraquarks, the Roper might be regarded as a cryptopentaquark: $[ud]\bar{l}$—$[ud]$ with $L=1$, and spin orientations given by $[-]\downarrow$—$[-]$ (conventions from the tables used). Of course we can only crudely approximate the mass of such particles by comparing it to others and glossing over any interaction between the diquark-antiquark. In particular the roper assignment might be seen, by noting the typical energies for an $L=1$ "good" nucleon, and assuming that the insertion of a good diquark has little energetic

cost even if more unstable, while subtracting some energy for the even-odd effect. In a similar way, we give a possible cryptopentaquark interpretation for other particles. Furthermore, these interpretation also fit consistently with possible interpretations of the recently possibly discovered $\Theta$ [40, 41, 42, 43] and $\Phi$ [44] pentaquarks. Besides that, however, the pentaquark assignment are mostly speculative and should be distinguished from the more compelling predictions of tetraquarks. They are listed in Tables 4.4.

# Chapter 5

# Conclusions, Future Directions

The evidence has been presented showing how a simple diquark interpretation produces a clean and consistent picture describing the structure and energies of hadrons.

Specifically, after classifying the particles according to this system, a simple paradigm emerges that can be summarized as follows. First, it is most fruitful to think of baryons most generally as a diquark-quark system, even so far as to describe ground states as a good diquark paired with a quark. The diquarks are described by their quark content and spin, and all combinations of different diquarks and quarks are to be expected with independent degrees of freedom (allowing for ground states to only have good diquarks). Good diquarks are lighter than their bad counterparts, with the effect diminishing for diquarks containing heavier quarks. The diquark behaves as an antiquark in color-charge, and thus for any rotating hadron we are to expect a Regge-like trajectory with a universal tension. Furthermore, there seems to be a large enough tunneling barrier between the diquark and quark that validates this Regge behavior down to $L = 0$, where diquarks might have huge overlap with the paired quarks; however in symmetric cases some tunneling is expected and observed. Finally spin-orbit and spin-spin (external to diquarks) forces play minor roles in the hadronic spectrum.

While I have presented evidence for these hypotheses mostly from the experimental data, and the clean consistency using a simple dynamical model, many of the fundamental reasons for their validity are not well understood. As such there are

many experimental and theoretical projects left to be done investigating the role of diquarks.

Experimentally, as has been suggested by Jaffe [27], a systematic exploration regarding the role of diquarks in deep inelastic collisions and distribution functions as well as scaling violations would greatly improve upon our understanding. Also, the particle classifications presented here immediately suggest the existence of several resonances as yet unseen or not well established. Likewise some resonances might actually exist at different energies than those listed in the PDG. Also the arguments presented, suggest tetraquark particles should exist beyond $L = 1$ although most probably quite narrowly. These predictions have been noted in the text, and should be searched out experimentally. Finally the question of exotics should be examined in the context of diquarks (as begun by Jaffe and Wilczek [34, 35, 36]), and the possibility of explaining several particles presented with possible cryptopentaquark or cryptotetraquark interpretation should be investigated. This is also an interesting project for lattice calculations.

Theoretically, a more sophisticated treatment of diquark correlations is greatly wanted. Related to this, such a project should seek to theoretically determine the effective diquark masses as extracted from the data. A better understanding might also open the way to investigating the possible diquark-antiquark interaction that would have to be present in pentaquarks. Once this is understood, then a similar analysis as the one presented in the text could be done as to determine at what angular momentum, if any, do the pentaquark states become energetically viable. Finally, a rigorous exploration of the tunneling barrier and mechanism should also be done. And in parallel, all these aspects might be investigated on the lattice.

Indeed diquarks seem to play a central role in the hadronic structure and spectrum. What resembles there signature appears to be written in the volumes of nature. It is an intriguing and exciting prospect that should yield new insight for QCD in understanding hadrons.

# Appendix A

# Chew-Frautschi Plots for Various Masses

Parametric plots of expression 2.10 reveal several characteristics. In general for the light mass regime as the sum of the masses grows or varies greatly, non-linear effects begin to emerge particularly in the low $L$ range, but in most cases the $E^2$ intercept (when plotted against $L$) is $\approx (m_1+m_2)^2$. However, for a robust range of masses ($m_1$, $m_2 \leq .5$ GeV) with reasonable values of $T$ fit from data ($1.1/(2\pi)$ GeV$^2$), the C-F plot continues to have a slope within about 10% of the massless case, and the plot remains essentially linear at and beyond $L = 1$. For the heavy mass regime, however, we find our results quickly breaks down with more significant deviances from linearity as $L$ grows. However, most of the resonances containing massive quarks currently exist only for small $L$. Several illustrative plots are shown in Figure A. Note that the plot of the very light masses case (a), is exactly in accordance with the analytic results derived from the expansions even at low $L$ (equation 2.12). For the heavy-light case (b), we see as mentioned more deviation from the reference line which contains half the slope of the massless case. However, part of this deviation is accentuated due to the fact that the first mass is not approximately zero. This was deliberately chosen to more realistically reflect possible resonances that fit this model. In the other two cases (c) and (d), the masses were selected to model possible quark or diquark effective masses. In these we see that the intercept is in agreement with $(m_1 + m_2)^2$.

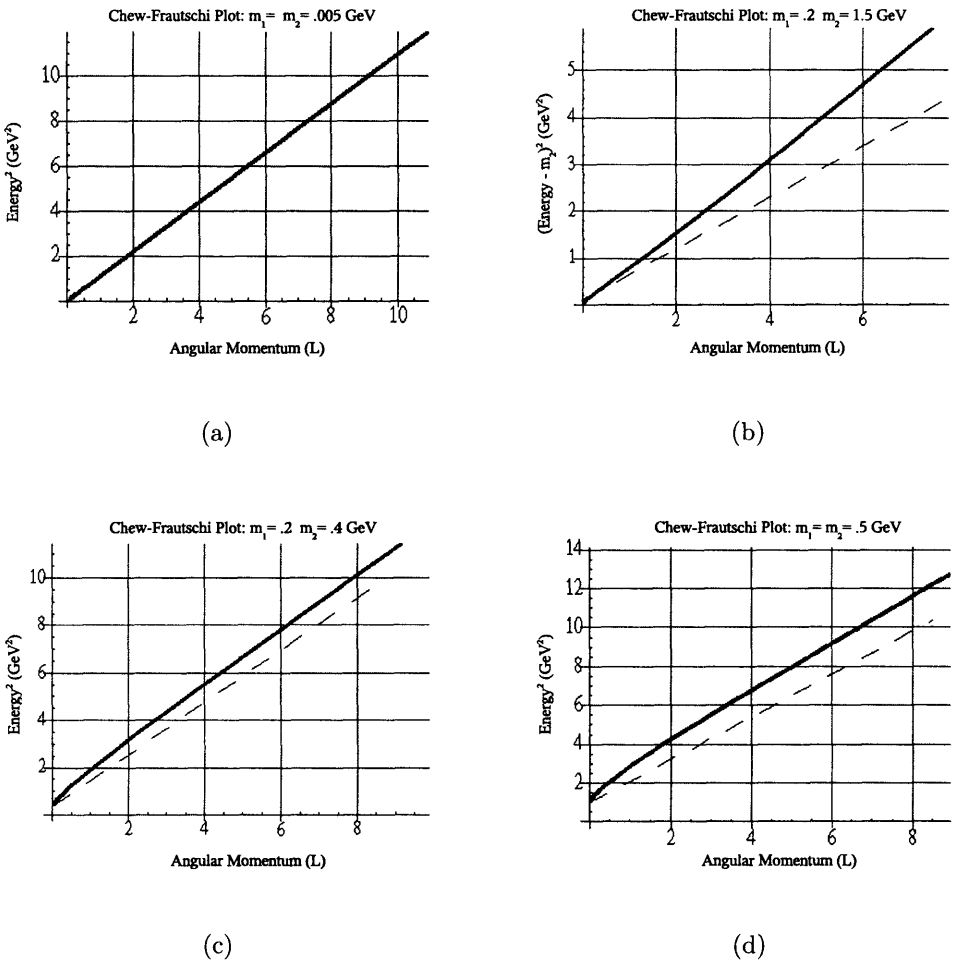


Figure A-1: Shown here are parametric Chew-Frautschi plots for various values of masses at the end of the string. The dashed line is motivated from the simple analytic solutions previously discussed and they are meant to serve as a reference. All cases are plotted with a string tension $T = 1.1/(2\pi)$ GeV$^2$ so as to produce a slope of 1.1 GeV$^2$. The reference line in cases (c) and (d) therefore have a slope of 1.1 GeV$^2$ and an intercept of $(m_1 + m_2)^2$. The reference line for plot (b) has a slope of 1.1/2 GeV$^2$. Note also that in case (b), $(E - m_2)^2$ has been plotted.

As expected especially for the more massive case (d), there is some non-linearity between $L = 0$ and 1, but the curves straighten to become parallel with the line shown for reference–which has the slope of the massless string, but the intercept given by $(m_1 + m_2)^2$.

# Bibliography


[1] Murray Gell-Mann. A schematic model of baryons and mesons. *Phys. Lett.*, 8:214–215, 1964.

[2] A. Selem and Frank Wilczek. Hadron systematics, diquark correlations, and exotics. In preparation.

[3] Thomas DeGrand. Recent developments from lattice qcd. 2005.

[4] F. Butler, H. Chen, J. Sexton, A. Vaccarino, and D. Weingarten. Hadron masses from the valence approximation to lattice qcd. *Nucl. Phys.*, B430:179–228, 1994.

[5] S. Godfrey and Nathan Isgur. Mesons in a relativized quark model with chromodynamics. *Phys. Rev.*, D32:189–231, 1985.

[6] D. P. Stanley and D. Robson. Nonperturbative potential model for light and heavy quark anti-quark systems. *Phys. Rev.*, D21:3180–3196, 1980.

[7] S. N. Gupta, S. F. Radford, and W. W. Repko. Semirelativistic potential model for heavy quarkonia. *Phys. Rev.*, D34:201–206, 1986.

[8] Stephen Godfrey and Jim Napolitano. Light meson spectroscopy. *Rev. Mod. Phys.*, 71:1411–1462, 1999.

[9] B. Rosenstein. Why the nonrelativistic potential model and the ultrarelativistic bag model give the same spectra. *Phys. Rev.*, D33:813–816, 1986.

[10] A. Chodos, R. L. Jaffe, K. Johnson, Charles B. Thorn, and V. F. Weisskopf. A new extended model of hadrons. *Phys. Rev.*, D9:3471–3495, 1974.

[11] A. Chodos, R. L. Jaffe, K. Johnson, and Charles B. Thorn. Baryon structure in the bag theory. *Phys. Rev.*, D10:2599, 1974.

[12] T. DeGrand, R. L. Jaffe, K. Johnson, and J. E. Kiskis. Masses and other parameters of the light hadrons. *Phys. Rev.*, D12:2060, 1975.

[13] C. Rebbi. Nonspherical deformations of hadronic bags. *Phys. Rev.*, D12:2407, 1975.

[14] P. J. Mulders, A. T. M. Aerts, and J. J. de Swart. Multi - quark states. 1. q**3 baryon resonances. *Phys. Rev.*, D19:2635, 1979.

[15] C. E. Carlson, T. H. Hansson, and C. Peterson. Meson, baryon and glueball masses in the mit bag model. *Phys. Rev.*, D27:1556–1564, 1983.

[16] John F. Donoghue and K. Johnson. The pion and an improved static bag model. *Phys. Rev.*, D21:1975, 1980.

[17] Andrius Bernotas and Vytautas Simonis. Towards the unified description of light and heavy hadrons in the bag model approach. *Nucl. Phys.*, A741:179–199, 2004.

[18] Peter Hasenfratz and Julius Kuti. The quark bag model. *Phys. Rept.*, 40:75–179, 1978.

[19] P. Gnadig, P. Hasenfratz, J. Kuti, and A. S. Szalay. The quark bag model with surface tension. *Phys. Lett.*, B64:62–66, 1976.

[20] K. Johnson and Charles B. Thorn. String - like solutions of the bag model. *Phys. Rev.*, D13:1934, 1976.

[21] K. Johnson and C. Nohl. A simple semiclassical model for the rotational states of mesons containing massive quarks. *Phys. Rev.*, D19:291, 1979.

[22] K. Jimmy Juge, Julius Kuti, and Colin Morningstar. Fine structure of the qcd string spectrum. *Phys. Rev. Lett.*, 90:161601, 2003.

[23] K. Jimmy Juge, Julius Kuti, and Colin Morningstar. Qcd string spectrum 2002. *Nucl. Phys. Proc. Suppl.*, 119:682–684, 2003.

[24] Mauro Anselmino, Enrico Predazzi, Svante Ekelin, Sverker Fredriksson, and D. B. Lichtenberg. Diquarks. *Rev. Mod. Phys.*, 65:1199–1234, 1993.

[25] A. De Rujula, Howard Georgi, and S. L. Glashow. Hadron masses in a gauge theory. *Phys. Rev.*, D12:147–162, 1975.

[26] D. Griffith. *Introduction to Elementary Particles.* Wiley, Canada, 1987.

[27] R. L. Jaffe. Exotica. *Phys. Rept.*, 409:1–45, 2005.

[28] S. Fleck, B. Silvestre-Brac, and J. M. Richard. Search for diquark clustering in baryons. *Phys. Rev.*, D38:1519–1529, 1988.

[29] Andre Martin. Regge trajectories in the quark model. *Z. Phys.*, C32:359, 1986.

[30] M. Iwasaki and Y. Marutani. Rotating bag model for hadrons. *Prog. Theor. Phys.*, 86:877–884, 1991.

[31] M. Iwasaki, N. Tanokami, and T. Nakai. Excited baryons in the mit bag model. *Phys. Lett.*, B314:391–396, 1993.

[32] S. Eidelman and et al. [Paricle Data Group collaboration]. Review of particle physics. *Physics Letters B*, 592:1+, 2004.

[33] A. Aktas et al. Evidence for a narrow anti-charmed baryon state. *Phys. Lett.*, B588:17, 2004.

[34] Robert L. Jaffe and Frank Wilczek. Diquarks and exotic spectroscopy. *Phys. Rev. Lett.*, 91:232003, 2003.

[35] Robert Jaffe and Frank Wilczek. Systematics of exotic cascade decays. *Phys. Rev.*, D69:114017, 2004.

[36] Robert Jaffe and Frank Wilczek. A perspective on pentaquarks. *Eur. Phys. J.*, C33:s38–s42, 2004.

[37] Colin Morningstar. Gluonic excitations in lattice qcd: A brief survey. *AIP Conf. Proc.*, 619:231–240, 2002.

[38] A. Vaccarino and D. Weingarten. Glueball mass predictions of the valence approximation to lattice qcd. *Phys. Rev.*, D60:114501, 1999.

[39] G. S. Bali et al. A comprehensive lattice study of su(3) glueballs. *Phys. Lett.*, B309:378–384, 1993.

[40] T. Nakano et al. Observation of s = +1 baryon resonance in photo-production from neutron. *Phys. Rev. Lett.*, 91:012002, 2003.

[41] V. V. Barmin et al. Observation of a baryon resonance with positive strangeness in k+ collisions with xe nuclei. *Phys. Atom. Nucl.*, 66:1715–1718, 2003.

[42] S. Stepanyan et al. Observation of an exotic s = +1 baryon in exclusive photoproduction from the deuteron. *Phys. Rev. Lett.*, 91:252001, 2003.

[43] V. Kubarovsky et al. Observation of an exotic baryon with s = +1 in photoproduction from the proton. *Phys. Rev. Lett.*, 92:032001, 2004.

[44] C. Alt et al. Observation of an exotic s = -2, q = -2 baryon resonance in proton proton collisions at the cern sps. *Phys. Rev. Lett.*, 92:042003, 2004.